DOT/FAA/TC-14/39

Federal Aviation Administration
William J. Hughes Technical Center
Aviation Research Division
Atlantic City International Airport
New Jersey 08405

Literature Review of Weak Adhesive Bond Fabrication and Nondestructive Inspection for Strength Measurement

August 2015

Final Report

U.S. Department of Transportation
Federal Aviation Administration

NOTICE

Technical Report Documentation Page

1. Report No.	2. Government Accession No.	3. Recipient's Catalog No.
DOT/FAA/TC-14/39		

4. Title and Subtitle	5. Report Date
LITERATURE REVIEW OF WEAK ADHESIVE BOND FABRICATION AND NONDESTRUCTIVE INSPECTION FOR STRENGTH MEASUREMENT	August 2015
	6. Performing Organization Code

7. Author(s)	8. Performing Organization Report No.
Michel D. Bode[1], Michael J Holle[1], and David Westlund[2]	

9. Performing Organization Name and Address	10. Work Unit No. (TRAIS)
[1]Sandia National Laboratories Airworthiness Assurance NDI Validation Center 3260 Spirit Dr. SE Albuquerque, NM 87106 [2]Federal Aviation Administration William J. Hughes Technical Center Aviation Research Division ANG-E281 Atlantic City International Airport, NJ 08405	11. Contract or Grant No.

12. Sponsoring Agency Name and Address	13. Type of Report and Period Covered
U.S. Department of Transportation FAA National Headquarters 950 L'Enfant Plaza North, SW Washington, DC 20024	Final Report
	14. Sponsoring Agency Code AFS-300

15. Supplementary Notes

The Federal Aviation Administration William J. Hughes Technical Center Aviation Research Division COR was David Westlund.

16. Abstract

The use of bonded repair doublers continues to increase in both metal and composite aircraft structures in small airplanes, transport airplanes, rotorcraft, and propellers. In general, bonded structures may include composite-to-composite, composite-to-metal, and metal-to-metal assemblies. Bonded structures will be even more important in transport airplanes as the new designs using extensive composite primary structures enter service. As the industry becomes more familiar with adhesive bonding technologies, their increased use for repair of metal structures is more likely. The development of appropriate inspections to determine the durability of bonded repairs over time is a requirement that is needed to maintain continued airworthiness. However, before advanced nondestructive inspection (NDI) can be fully developed and validated, a mechanism for repeatedly producing large numbers of reduced-strength bonded-repair doubler test specimens must be developed. This project investigated and developed one method of fabricating controlled, reduced strength, aluminum bonded repairs. Additionally, literature was reviewed and emerging NDI methods to measure bond strength quantitatively were investigated.

17. Key Words	18. Distribution Statement
Adhesive Bonds, Fabricating weak bonds, Nondestructive inspection, NDI, Bond-strength measurement	This document is available to the U.S. public through the National Technical Information Service (NTIS), Springfield, Virginia 22161. This document is also available from the Federal Aviation Administration William J. Hughes Technical Center at actlibrary.tc.faa.gov.

19. Security Classif. (of this report)	20. Security Classif. (of this page)	21. No. of Pages	22. Price
Unclassified	Unclassified	92	

ACKNOWLEDGEMENTS

Many people contributed to this work and deserve thanks. David Galella from the Federal Aviation Administration (FAA), William J. Hughes Technical Center Maintenance and Inspection program funded the work. Dr. John Bakuckas, FAA Structures and Materials Section, facilitated interactions with industry participants. Many people from The Boeing Company, including Russell Keller, Bud Westerman, Kelly Greene, Carly Brewer, Michael Evens, A. Josh Slocum, and Megan Watson, fostered the work and provided technical guidance on fabrication of intentional weak bonds. At Sandia National Laboratories, Mark Marrujo, Carl Jacques, Todd Sokol, and Josh DeReu set up the bonding lab, developed the bonding procedures, and executed all of the bonding and mechanical strength testing work.

TABLE OF CONTENTS

LIST OF FIGURES

LIST OF TABLES

LIST OF ACRONYMS

AANC	Airworthiness Assurance NDI Validation Center
AFRL	Air Force Research Laboratory
CCA	Controlled contamination area
CFRP	Carbon fiber-reinforced plastics
EIS	Electrochemical impedance spectroscopy
FAA	Federal Aviation Administration
IPA	Isopropyl alcohol
IR	Infrared
LBI	Laser bond inspection
LLW	Leaky Lamb waves
NCATS	Noncontact acousto-thermal signature
NDI	Nondestructive Inspection
NDT	Nondestructive testing
PAA	Phosphoric acid anodization
SNL	Sandia National Laboratories
SWF	Stress wave factor
TRL	Technology readiness level
TSA	Thermoelastic stress analysis
USAF	United States Air Force
UT	Ultrasonic testing

EXECUTIVE SUMMARY

The use of bonded repair doublers continues to increase in both metal and composite aircraft structures in small airplanes, transport airplanes, rotorcraft, and propellers. In general, bonded structures may include composite-to-composite, composite-to-metal, and metal-to-metal assemblies. Bonded structures will be even more important in transport airplanes as the new designs using extensive laminated composite principle structures enter service. As the industry becomes more familiar with composite and adhesive bonding technologies, their use for repair of principal load-bearing structures is likely to increase. Development of appropriate inspections to determine the durability over time of bonded repairs is a very high priority. Direct, nondestructive measurement of bond strength is essential for maintaining continued airworthiness of both composite and metallic bonded repairs with the required level of aviation safety. However, before advanced nondestructive inspection can be fully developed and validated, a mechanism for repeatedly producing large numbers of controlled, reduced-strength, bonded repair test specimens must be developed.

1. INTRODUCTION

1.1 BACKGROUND

1.1.1 Adhesive Bonding Technology

The aerospace industry uses organic synthetic polymer adhesives for many applications. Because the adhesives are organic and have a lower specific gravity than most (metal) adherends, the overall density of a structure can be reduced significantly while maintaining structural integrity to carry ground and flight loads. From the structural integrity perspective, there are good reasons to replace riveted structure with adhesively bonded structure, the most notable example being the removal of stress concentrating fastener holes and the distribution of loads across the entire bonded joint, thus reducing the potential for fatigue cracking. However, because of the relatively high modulus of elasticity, adhesive bonds are prone to disbonding. Disbonding is defined as the inability to transfer loads across an interface regardless of whether the bonding faces are in contact or not. Many adhesively bonded structures are already in use in both metallic and composite airplanes, and it has become increasingly apparent that adhesive bonded repairs of composite laminate principal structural elements are essential to the long-term viability of these new airplane designs. The main impediment to implementing bonded repairs in general is the lack of means to nondestructively measure bond strength. Without actual bond-strength values, structural engineers cannot calculate projected life estimates of bonded structures, thus limiting their ability to prove continued airworthiness of the structure. While adhesive bonding processes during manufacturing are considered well controlled, bonds made during repair processes are more often subject to process variations, which can cause substantial degradation in bond strengths. Accordingly, measuring and validating adhesive bond strength nondestructively after repair is essential for both metal and composite structures. The goals of this report are: to analyze methods that have been used by other researchers to create intentional weak bonds; to review methods currently used to measure bond strength nondestructively and work done to improve or develop new methods; and to develop a test plan for making controlled-strength weak bonds to support nondestructive inspection (NDI) development and validation of bond-strength measures.

Adhesive bonding is an alternative to more traditional mechanical joining methods used in aerospace applications, such as riveting. The assemblies created by the adhesive bonding method of joining materials are called adhesive joints or adhesive bonds. The adherends are the solid materials (aluminum or composite) being joined by the adhesive. The phenomenon that allows the adhesive to transfer a load from the adherend to the adhesive joint is called adhesion. The actual strength of an adhesive joint is primarily determined by the mechanical properties of the adherends and the adhesive [1]. While individual adhesives will vary in their mechanical properties and the chemistry used to create them, there are general chemical classes that can be considered. The most common class for aerospace applications is epoxy adhesives.

In general, there are five basic requirements for achieving durable adhesive bonds:

1. Properly preparing the substrate surfaces for bonding
2. Correctly mixing and applying the adhesive materials
3. Controlling the bond line thickness
4. Applying uniform and correct clamping pressure during cure
5. Properly curing the adhesive with correct temperatures and times

Discussions later in this paper will address how variations from ideal requirements might be used to generate weak bonds in a repeatable way. The following sections provide some background to help the reader understand some of the basic science behind adhesive bonding and how variations from ideal bonding requirements can affect bond integrity.

1.1.2 Physical and Chemical Properties

Adhesives, especially those used in aerospace, are generally organic polymeric materials that exhibit viscoelastic properties, meaning they have both viscous and elastic properties. Polymer adhesives are organic materials that undergo a polymerization (molecular cross linking) reaction upon reaching the thermal transition temperature to become a thermoset plastic. Polymer adhesives are characterized by a distribution of polymer chain lengths that undergo some degree of cross-linking between chains, and the degree of cross-linking between chains has an influence on the properties. The entanglement molecular weight is the point at which the polymer chains have become so intertwined that pulling on a single chain also pulls on a substantial number of adjacent chains. Once the adhesive becomes the high-molecular-weight distribution thermoset plastic, it exhibits linear viscoelastic properties. Thus, the material response to temperature and the rate of stress application are dominant factors that characterize its performance as an adhesive. Polymer adhesives can be classified by their response to stress, for which high molecular weight, due to a high degree of polymerization, provides a brittle adhesive with high elastic modulus; whereas a low molecular weight adhesive provides a tough (rubbery) adhesive with a low elastic modulus due to less polymerization. Brittle, high-modulus adhesives are generally desirable for efficiently transferring loads across a joint. Thermosets are sometimes considered to possess nearly infinite molecular weight and, therefore, usually exhibit brittle viscoelastic properties. Considering the above information for thermosetting systems, there is a complicated relationship between the cure cycle—the time and temperature cycle to which the thermoset resin is subjected—and the physical state of the thermoset. The time–temperature–transformation diagram must be used when selecting an adhesive material and designing a fabrication recipe.

1.1.3 Mechanical Properties

When properly designed and built, adhesive joints do not exhibit the high stress concentrations observed in fastened joints. However, they do require a much larger surface area of contact between the adherend and the adhesive than the fastened joint to carry the same load. The concepts of elastic modulus, elongation, fracture resistance, and common loading forces are basic to understanding the mechanical properties of adhesive bonds. The three types of forces typically applied to adhesive joints are tensile loads, shearing loads, and cleavage loads.

When considering tensile forces, the concepts of stress–strain plots, Young's modulus, elastic linear response, plastic deformation, and Poisson's ratio are all important. The tensile stress is used to calculate the stress–strain curve, from which Young's modulus and Poisson's ration can be derived. During elastic deformation, a material returns to its original shape when the stress is removed, and it does so without the loss of mechanical energy as heat. During plastic deformation (from the yield point up to breaking at the ultimate tensile strength), the material is absorbing energy, which becomes heat upon material deformation and breaking. Adhesives (which are considered stiff materials) typically possess a high Young's modulus and lower values of Poisson's ratio (around 0.25).

When considering shear forces, a similar situation arises. The shear stress and shear strain are plotted, which leads to the shear modulus value of the material, similar to a tensile modulus. Both the tensile and shear modulus can be related to the Young's modulus and the Poisson's ratio through a simple ratio calculation.

Strain energy density is calculated as the area under the stress-strain curve. Ultimate strain energy density is a parameter of the adhesive describing how much mechanical energy can be absorbed before failure. Adhesives that are stiff enough to support the design load with a high ultimate strain energy density are desirable. Polymer-based adhesives absorb mechanical energy applied to the joint and dissipate that energy as heat because of their viscoelastic properties. The mechanical energy absorbed when the load is applied can be dissipated as heat in the adhesive without breaking the bond. The degree of heating is influenced by the entanglement molecular weight within the polymer and by the degree of heterogeneous cross linking between the adherend and adhesive at the interface.

Young's modulus, shear modulus, Poisson's ratio, strain energy, and the critical strain energy release rate are important quantities to consider in understanding the mechanical properties of adhesives. Additionally, the most important viscoelastic parameters are defined as the storage and loss moduli. These factors are critical in the design and selection of adhesives to prevent a cohesive failure (bond failure within the adhesive film itself). However, the assumption is made that the correct adhesive has been selected for an application; thus, adhesive failure (bond failure at the interface between adherend and adhesive) becomes the dominant failure mode to guard against. Determining the strength of the bond at the adherend/adhesive interface becomes the major issue, for which NDI methods have not yet been fully developed.

1.1.4 Adhesively Bonded Repairs

Historically, most repairs to aircraft structures have been attached with fasteners, similar to those used on the rest of the aircraft, principally rivets and bolts. Increased weight and the creation of additional holes to the structure are undesirable outcomes of fastened repairs. Thus, the aerospace industry continues to seek alternative methods for fastened repairs. Adhesively bonded repairs are a method of intense interest because they add less weight, distribute loads over the entire repair area (thus reducing the potential for high stress sites that can initiate cracks), and do not require the creation of holes in otherwise good structures. The use of bonded repair doublers continues to increase in both metal and composite aircraft structures in small airplanes, transport airplanes, rotorcraft, and propellers. In general, bonded structures may include composite-to-composite, composite-to-metal, and metal-to-metal assemblies. The

increased-use bonded repairs for principal load-bearing structures is also more likely as the airplane maintenance industry becomes more familiar with composite and adhesive bonding technologies. Bonded repairs will be even more important in new transport airplane designs using extensive laminated composite structures. Therefore, the development of NDI techniques to determine bond repair durability over time is a high priority. Direct, nondestructive measurement of bond strength is essential to maintaining continued airworthiness of both composite and metallic bonded repairs with required levels of safety. Current NDI technology is not able to obtain a continuous measure of bond strength. Proof loading inspection methods have been developed, but these simply indicate that a bond is providing adequate load transfer at or below a given strength level. Advances in ultrasonic and thermographic NDI show some promise for eventually providing material property measurements that may be correlated to load transfer strengths. However, progress has been slowed by the dearth of available specimens appropriately simulating the defective bonded repair condition. Each researcher tends to develop his or her own specimens, with highly variable and unsubstantiated bond-strength results. In reviewing recent results, it is not always obvious how a particular specimen fabrication method is related to actual bonded repair specimens (or even newly fabricated structures). In some cases, the final strength of bonded specimens is assumed and not substantiated by mechanical strength measurements. Before advanced NDI can be fully developed and validated, a mechanism for repeatedly producing large numbers of controlled, reduced-strength, bonded repair test specimens must be developed and implemented. Only then can NDI researchers be assured of having specimens that represent realistic weak bond conditions found in the fleet, and, equally important, be able to provide industry with a mechanism to gauge the effectiveness and cost of any particular NDI method that is developed.

1.2 PURPOSE

This project is intended to support the development and implementation of adhesive bond-strength measurement in transport airframe structures by NDI methods. It is part of an overall industry goal to support continued airworthiness of bonded repairs on transport airplanes through damage-tolerance methods, such that inspection start points and repeat intervals can be determined. The goal of this report is to analyze methods that have been used by other researchers to create intentional weak adhesive bonds, review methods currently used to nondestructively measure adhesive bond strength, review work done to improve or develop new methods, and develop a test plan for making controlled-strength weak bonds to support development and validation of NDI bond-strength measurements. Part of the overall goal includes developing statistical evaluation methods to measure the reliability of such bond-strength inspections.

1.3 TASKING

While adhesive bonding materials and methods continue to improve and become more standardized, their implementation in the aerospace maintenance sector requires a high level of process control relative to other aviation repair processes. Maintenance and repair technicians are familiar with, and very skilled at, performing work in accordance with aerospace industry standard practices detailed in such references as structural repair manuals. However, with adhesive bonding, the number of critical steps with exacting processing requirements is extensive. Additionally, process parameter changes that appear to the repair technician as being

relatively minor deviations may cause major changes to the final structures. One good example is that a relatively small change in cure temperature ramp-up rates may cause major differences in the polymer matrix cross-linking, resulting in substandard bond-strength levels and transition from adhesive to cohesive bond failure mode. The implication is that to achieve repeated bonds with highly controlled strength values, the development of relatively exacting processes by personnel trained to understand and guard against any excursion from established procedures is required. Thus, the Airworthiness Assurance NDI Validation Center (AANC) developed a research plan predicated on four major tasks, detailed below, to achieve the overall goal of improving the state of the science of NDI for bond-strength measurement. Within the overall task framework, 14 distinct subtasks, detailed below, were cited as necessary steps.

1.3.1 Tasks

1. Fabricate both "good" and "weak" adhesively bonded metallic repair specimens.

2. Test the mechanical properties (strength and failure mode) of adhesively bonded metallic repairs to substantiate bond fabrication methods.

3. Develop, and provide sets of "good" and "weak" adhesively bonded metallic repair specimens to industry to support NDI method development of quantitative bond-strength measurement.

4. Perform reliability assessments of NDI methods for bond-strength measurement methods using additional specimen bond sets fabricated at the AANC.

1.3.2 Subtasks

1. Perform a literature review of adhesive bonding technologies, specimen testing methods, and NDI methods for assessing adhesive bond strength.

2. Quantify or rank the potential of advanced NDI methods to measure bond strength in weak bonds.

3. Coordinate with Federal Aviation Administration (FAA) William J. Hughes Technical Center structural integrity researchers in the FASTER laboratory and with other researchers to leverage associated work to maximize benefits and learning from the program.

4. Assess various fabrication methods for building coupon specimens with a range of controlled, quantified bond strengths in aluminum-to-aluminum specimens.

5. Select a subset of fabrication methods and build sets of specimens (aluminum-to-aluminum and composite-to-aluminum) for bond strength testing.

6. Perform load testing to determine the ranges of bond strengths obtained by each fabrication method. Repeated inspections may occur during load testing if it is apparent that partial bond failure is occurring that would provide an opportunity to further assess an NDI method.

7. Analyze load testing data relevant to the fabrication methods, looking for correlation of specific fabrication factors with generation of repeatable reduced-strength bonds.

8. Select appropriate NDI methods for assessment of bond strengths in fabricated specimens.

9. Perform NDIs of specimens for bond-strength quantification prior to destructive mechanical load testing.

10. Analyze inspection results looking for correlation with, and sensitivity to, bonds with reduced strength.

11. Work with NDI equipment vendors to enhance the methods that show the most promise for measuring bond strength.

12. Simultaneously use the NDI methods selected to inspect composite (i.e., boron epoxy) for aluminum test samples to detect reductions in bond strength.

13. Determine the appropriateness of aluminum-to-aluminum fabrication methods for application on composite-to-aluminum specimen fabrication.

14. Continue to build and test specimens, as needed, to refine both the fabrication processes for repeatability and the NDI methods for better sensitivity.

2. LITERATURE REVIEW

More than 200 individual papers were reviewed as part of this work. Two major areas of interest considered were intentional weak bond fabrication and NDI for bond strength measurement. Papers were sorted into the two categories of interest and a short synopsis of each was included in a separate Excel™ database. Full papers were then requested and reviewed for a subset of the papers that appeared to have information specifically pertaining to weak bond fabrication methods and/or NDI for bond-strength measurement. All papers cited in this work are listed in the references section. Papers reviewed but not cited in the paper were included in appendix B.

2.1 WEAK BOND FABRICATION METHODS

Researchers in materials and aerospace have investigated the properties of bonded materials with the engineering goal of fabricating higher quality bonds; in doing so, they have identified critical factors affecting bond quality. Knowledge of such factors allows fabrication of intentional weak bonds to proceed with greater efficiency. By using this basic knowledge, many NDI developers have attempted to simulate defective bond conditions to support development of bond-strength measurements by nondestructive methods. Reviewing the literature reveals that, although weak

bond fabrication has been conducted along the lines of five or six main functional bonding steps, little repetition has occurred in specific fabrication methods. Researchers tend to develop specimens specific to the structural designs and defect problems, which in turn dictates the NDI method to be employed. The specimens built to date tend to be unique articles for specific purposes instead of generalized or multipurpose reference standards. While there is a need for specimens that are useful for investigating the wide range of weak bond conditions to facilitate NDI development and validation, it is equally true that development of a general reference specimen for bond-strength assessment is a difficult task. Because of the complexity of causes that lead to weak or deteriorated bonds, it may not be possible to develop just one specimen, but will likely require sets of specimens with a variety of defects for each of the major material systems. In fact, the need for appropriate specimens has inhibited the development of NDI methods that show promise for bond-strength measurement. When defect specimens are different in terms of how they are made and actual bond-strength values remain unverified or are determined with different tests, it is extremely difficult to gauge the accuracy and precision of reported bond-strength measures obtained by any given NDI method. Further, without standardized specimen sets, there is no opportunity for comparison across methods. Typical NDI equipment vendors depend on their customers to provide specimens for method development and, in this case, there are no industry standard specimens. There are proprietary specimens and designs for solving narrowly defined problems of a particular manufacturer but no way for the rest of the industry to gain insight that could lead to large-scale solutions based on fundamental principles. One goal of this paper is to foster a higher level of understanding of 50 years of adhesive bond NDI research and promote the realization of bond specimens useful for both NDI development and validation efforts across a broad array of material systems being used in transport aircraft today.

2.1.1 Definition of Weak and Kissing Bonds

Weak bonds can be defined in many ways, but for the purpose of developing NDI methods to assess bond strength, consensus among researchers has generally evolved into a common set of characteristics that center on failure of the adherend/adherent interface. Although failure of the adhesive material (cohesive failure) can occur, it is considered a design-related failure that is fixed by selecting another more appropriate adhesive material with the proper strength values for the particular application. The concern of the structural integrity community centers on bonded structures that may have a range of bond strengths from nearly full strength, degrading into partial strength bonds, and ending with very low- or no-strength bonds. In particular, the term “kissing bonds” has been adopted by the research community to describe a bonded structure for which contact is intimate between both adherends and the adhesive, but there is no residual bond strength for at least one interface. Marty et al. [2] offers a functional definition of a kissing bond. The criteria are 1) the bond strength in peel must be less than 20% of full strength; 2) the failure mode must be 100% adhesive; and 3) a normal incidence L-wave ultrasonic signal must not exhibit low-signal attenuation (i.e., the structure must transmit the ultrasonic testing (UT) signal across the kissing bond as if no disbond was present). Additionally, a theoretical definition of a kissing bond is when the adherends are in full physical contact, as if bonded, but the interface between adherends provides no mechanical load transfer capability. Further, the type of load (i.e., tensile, shear, or peel) that is being applied is consistent with the application of the bond.

Numerous ways are found in the literature for generating weak bonds in both metallic and composite substrate systems. Surface preparation process variables, including contamination, mixing ratios, adhesive application, bond line thickness variations, and processing or cure deviations from an optimum, are the main steps undergoing variation to fabricate intentional weak bonds. The methods for metallic and composite substrate bonding often differ; this is particularly so in the early surface preparation steps. However, the general steps can be classified in the same way. A good example are the differences in surface treatments and processing steps required to form a strong, durable adhesive bond with metal versus carbon fiber composite systems. Cleaning and surface activation steps are common to both materials, but best results are obtained in much different ways.

2.1.2 Surface Preparation Including Contamination

Of the major issues commonly discussed for ensuring a quality adhesive bond, surface preparation is the highest priority for metal bonding. Preparing mechanically active sites on the adherend so that they provide high-surface free energy is the goal. This includes creating optimal surface roughness and ensuring that the surface is free from contaminants, such as dust, oils, and other chemicals. This is true whether a composite-to-metal or a metal-to-metal configuration is undergoing bonding. If carbon fiber composite patches are being bonded to aluminum, then special care must be taken to prevent galvanic corrosion of the aluminum because it is more anodic on the galvanic scale than carbon fiber. The other main issue that must be addressed is the preparation of the metal substrate to provide a good chemically clean bonding surface. The methods for generating weak bonds for composites often differ from those used for metals because of the differences in the surface preparations involved in forming an adhesive bond. However, in principle, the concepts are the same even though the steps are performed differently.

2.1.2.1 Metal/Aluminum Adherends

McCray et al. [3] were searching for a replacement for chromate primers. They used common aerospace adhesive bonding materials and systems. The strength of bonds was tested with tensile lap shear specimens, per ASTM D1002. The authors found variable results consistent with prior work, indicating many variables can influence adhesive bond strength. This is a good baseline paper for understanding adhesive materials, processes, and strength-testing methods.

Lefebvre et al. [4] studied the effect of different substrate surface pre-treatments on the initiation of interfacial fatigue cracks studied for adhesive bonds. Aluminum-epoxy specimens were used to investigate how surface pre-treatment affects resistance to fatigue crack initiation at the interface corner. The effect of four different treatments — P2 etch, phosphoric acid anodization (PAA), sulfuric acid anodization (SAA), and sol-gel —was investigated in a bimaterial system with a 90 degree epoxy wedge test under sinusoidal cyclic loading. The surface treatment effect was rather significant on the resistance to fatigue crack initiation at the interface. Results show that PAA generated the strongest interface, while SAA led to the weakest.

Tracey et al. [5] performed a study to determine the effect of many variables on contact angle measurements for peel ply composite surfaces. Two significant outcomes were that contact angle measurements will vary with time depending on the fluid used, and peel ply orientation produces differing contact angle measurements. The overall conclusion was that studying

contact angle measurements as a way of measuring surface energies is sensitive to many variables. In related work, Dillingham et al. [6] discuss the relationship of surface properties to adhesion and give examples in both metal and composite systems. Surface morphology (mechanical interlocking and contamination tolerance), surface composition (wettability and chemical bond formation), contact angle, surface energy, and fracture toughness are presented and related to bonding theory. The Surface Analyst Tool™ and its features are presented as a means to assess contact angle. The authors provide data from various examples and present data to show that the tool can quantitatively correlate to adhesive joint strength, toughness, and failure mode, and be sensitive to contamination levels below those levels affecting adhesive joint performance. This is a good general paper to understand the principles used by Brighton Technologies in development of the Surface Analyst Tool™ for measuring goniometer-based surface free energy levels in composite adherends. In this work, they detected peel-ply-derived siloxane contaminants and showed that a readily detectable threshold amount of contamination is required to affect fracture toughness, and that the amount is similar for several distinct adhesive systems.

The Boeing sol-gel process (Boegel-EPII) is an organosilane surface preparation method for metallic substrates for adhesive bonding and painting applications. Liu et al. [7] investigated the effect of processing conditions on adhesion strength and durability of a sol-gel reinforced, rubber toughened epoxy-aluminum joint. The authors are from Lehigh University and The Boeing Company, both recognized leaders in aerospace aluminum bonding technology. They made their own resins and mixed the adhesives from base chemicals. Using an asymmetric double cantilever beam (ADCB) wedge test, the adhesion of the sol-gel reinforced epoxy-aluminum joint in a humid environment was measured as a function of sol-gel processing conditions. Three factors showed good correlation with bond strength: a) sol-gel drying time, b) sol-gel concentration, and c) humidity during sol-gel drying. Prolonged drying times led to a decrease in fracture energies. Peak fracture energies were achieved at 75 minutes of drying time. The critical and threshold fracture energies show different trends as sol-gel concentration varies. Better adhesion performance was seen for sol-gel dried at higher humidity compared to lower humidity. Overall, observed trends for adhesion performance can be explained in terms of interdiffusion of the sol-gel film and epoxy. The diffusion of epoxy into the sol-gel layer is hypothesized to strongly depend on the degree of condensation of the sol-gel film and is directly affected by the sol-gel processing conditions. A highly condensed sol-gel layer limits the interdiffusion with the epoxy adhesive. However the resulting fracture energy is not a linear function of any one variable and is, therefore, not easily predicted. Regardless, this paper directly supports the hypothesis that sol-gel variations can be used to make controlled-strength weak bonds in simulated bonded aluminum repairs.

Other researchers have also explored the effects of organosilane variations on bond strength in aluminum joints. Marty et al. [2] and Abel et al. [8] explored the effects of organosilane surface treatment variations on bond durability in aluminum. They found a range of application and film condition parameters that contribute to joint durability. Parameters relating to organosilane solvent type, solution concentration, pH, and hydrolysis time can influence durability. Other parameters, such as film-drying temperature and in-process time delay, had little effect on their studies, yet Liu et al. [7] reported significant effects. Abel et al. [9] also studied the effects of wet and dry environments on fatigue cycling results and found increases in bond durability

associated with organosilane pretreatments. Underhill and DuQuesnay [10] found that joints without silane pretreatment were an order of magnitude less durable in fatigue tests than silane treated joints. Additionally, the *R*-ratio of fatigue tests had a substantial effect on silane-treated joints. Clearly, organosilane (whose trade name product is Boe-Gel®) treatment variations offer huge potential to fabricate reduced-strength bonds with the level of control to tailor the bond-strength values. By controlling the aforementioned parameters, the strength of an adhesive bond can be tailored, making it another suitable technique for generating repeatable bonds with controlled strength levels.

Applying contamination in some manner to a substrate is another method for generating weak bonds. Generally speaking, this alters the surface chemistry and inhibits a good bond from being formed. For example, Jeenjitkaew et al. [11] investigated changes in morphology and surface chemistry across a bonded area with one surface of an aluminum joint contaminated by the following: a semi-permanent mold release agent (Frekote); an artificial eccrine perspiration (human sweat); cutting oil lubricant; and, in a companion paper, ElectRelease™. Results were variable, depending on the contamination applied, but were generally successful in fabricating reduced-strength bonds. Bonds made with ElectRelease™ were at 57% of full strength and showed adhesive failure mode.

Leclerc et al. [12] focused on making and inspecting kissing bonds using aluminum plates. Consistent kissing disbonds were fabricated by applying a diluted release agent to primed aluminum surfaces. Bonding of aluminum plates was done with AF-163K and FM300 film adhesives using standard processing parameters. Bond samples were inspected with conventional UT, flash thermography, vibrothermography, and laser shearography with non-conclusive results.

Marty et al. [2] used a dry layer of silicone in place of primer on aluminum. In the same study, an electrically disbonding epoxy was also used to create weak (kissing) bonds. The properties of this epoxy are such that, once bonded, it can be unzipped by applying an electric field. It was observed that, despite tight control of the applied voltage and duration of the application, the resulting disbond was always too strong to be representative of a real kissing bond. Yang, Y. et al. [13] simulated weak kissing bonds by applying a thin layer of mold release wax on an aluminum substrate. In another large research effort conducted at Sandia National Labs (SNL) [14] for the automotive industry, more than 30 methods were evaluated for generating weak bonds, including various levels of grease thickness, grease with thinner layers of adhesive, different mold releases with various amounts of coverage, diluted mold release, non-optimum cure profiles, hot-wet conditioning, applications of different contaminants (i.e., water, wax, sand, Vaseline®), oil application with various levels of coverage, less than 100% adhesive coverage, and baking powder with various levels of coverage. In general, contamination can be an effective method for creating weak bonds; however, often the challenge is controlling the amount of contamination and getting repeatable results.

Underhill et al. [15] found that fatigue life depended on surface preparation of the bonds in aluminum using FM73 epoxy adhesive. There was also a correlation between wedge test and fatigue life performance. Warm water pretreatment of aluminum prior to silane treatment increased wedge test performance. There are numerous surface preparation methods, so care

should be exercised when exploring the large variety of treatments that can be devised. This work validates the use of wedge testing as an acceptable method to measure bond strength and durability.

In one recent study, Barroeta-Robles et al. [16] used two approaches to form controlled strength (weak) bonds on aluminum substrates. In the first approach, the substrate was treated with a chemically modified primer based on functional silane coupling agents to achieve selective interactions between the adhesive and the substrate. These coupling agents bond strongly to the substrate surface but can be selected so as to have varying degrees of coupling with the adhesive. By controlling the silane mixture, the resulting bond can be controlled to be weaker than the optimum bond strength of the adhesive. The results of this work were promising because the authors were able to achieve repeatable controlled strength bonds. In the second approach, the chemical reaction and degree of chemical conversion of a commercial two-part adhesive was reduced, resulting in decreases in bond strength and in other material and mechanical properties for the system. While other researchers have modified paste adhesives by reducing hardener content, this approach was to balance the reduction in cross linking monomers by including an additional component to convert 100% of reactive epoxy bonds in the adhesive while limiting the coupling interactions between the adhesive and the substrate. The resulting adhesive has property stability with time, such that bond strength does not vary between specimen manufacture and inspection sites. While this approach is effective only for two component paste adhesives, the modification can be applied to multiple substrates and on any primer treatment. The results from this work were also promising because a change in failure mode was observed below a certain threshold amount of hardener.

Biegert [17] looked at six different non-ODC (ozone-depleting chemicals) cleaners used for aluminum preparation prior to bonding or painting. The tapered double-cantilever beam test was used to evaluate bond line fracture toughness. The bottles of cleaners were stored in varying conditions, simulating best- and worst-case scenarios (i.e., best: 22 C, 10% RH, dark room vs. worst: 40 C, 50% RH, fluorescent lighting). A selection of aluminum samples was cleaned using the cleaners, while the others had grease applied and were then cleaned. Bond line fracture toughness changed dramatically for cleaners stored in harsh conditions for more than 13 weeks; this was thought to be due to changes in moisture content and the polarity of the cleaners.

2.1.2.2 Composite Adherends

Kinloch and Kodokian [18] demonstrated that abraded and solvent wiped thermo plastic-based fiber composite material adhesive bonds were much weaker than corona discharge prepared surfaces. Adhesive fracture energy $G_{(c)}$ values were obtained by double-cantilever beam joint testing. Solvent wiping may thus provide a reliable method of generating weak bonds in carbon fiber-reinforced plastics (CFRP) laminates, although the control and repeatability of the technique must be established.

McDaniel et al. [19] discussed specimen designs as well as durability testing and results for bonded composite samples. This, however, is an early review of proposed work and no contaminated weak bond samples were actually made. Future work will fabricate composite specimens using masks to vary the level of contaminants. Authors also discussed electrochemical sensor analysis if the peak current flow in a current/voltage (CV) plot

corresponds to maximum electrochemical activity and potential contamination. The CV results for limited early test samples correlate with fracture energy values, although data were not presented. The CV method could provide one way to measure bond strength in composite specimens.

Chamochin et al. [20] found that glass reinforced plastic composite specimens treated with atmospheric plasma showed a reduction in mechanical properties, resulting in adhesive failure. The durability was tested using the wedge test. Specimens treated with atmospheric plasma also showed a lower durability than the other surface treatments.

Bossi et al. [21] varied surface preparation of CFRP laminate specimens to generate full-strength and weak bonds. Variables included grit blast, sanding, as-tooled with solvent wipe, and peel ply removal. Peel ply variables included silicon release blue, nylon, and polyester materials. Contamination of surfaces with mold release prior to bonding was also used to make weak bonds by both Bossi et al. [21] and Ecault 22].

In work by Yang, S. et al. [23], weak bonds were formed by sanding only certain fractions of the total surface area of the composite substrate for high strength, and not sanding others for weak strength. In other work, Perton et al. [24] created relatively weak bonds by treating some of the carbon fiber reinforced epoxy bonding surfaces with corona discharge. In work by Dillingham et al. [25], diluted solutions of siloxane were applied to peel ply, which was then applied to composite laminates to create various levels of contamination.

2.1.3 Mixing and Applying Adhesives

Most of the current work with adhesives for aerospace bonding employs the use of pre-mixed adhesive films. This eliminates the potential for mixing and applying process control excursions. Not much recent work was found for which researchers were mixing their own formulations of adhesives. While there is likely a great number of ways adhesives could be mixed to achieve weak bonds, they are not realistic fabrication methods because the failure mechanisms may be very different from those encountered in actual service.

Barroeta-Robles et al. [16] performed work that resulted in repeatable weak bonds on aluminum plates using two methods: tailoring the silane primer chemistry, and varying the mix ratios of Cytec FM73 and Hysol EA9394 adhesives. They also performed solvent wipe after grit blast, which is not recommended by industry experts, and nitrogen blow off, which is recommended. The failure mode transition from cohesive to adhesive for lap shear specimens showed strength reductions to less than threshold values. The authors recommended the use of double-cantilever beam testing as the preferred strength measurement method.

Bossi et al. [21] created weak bonds of 100%, 62%, and 33% relative strength in composite laminate specimens through the poor mixing of the epoxy adhesive, inappropriate surface preparation, and controlled contamination. Full, 75%, and 50% bond-strength specimens were made by mixing a commercial two-part epoxy in hardener to resin ratios (B/A) of B/A=0.17 (standard), 0.05, and 0.03, respectively.

2.1.4 Bond Line Thickness Variations

Davies et al. [26] determined that thicker bond lines reduced joint strength in tensile loading. They recommended keeping epoxy adhesive joints in aluminum substrates to less than 0.8 mm (0.032″) thick. The implication here is that by making thicker bond lines, the strength of the bond could potentially be reduced, but it is unclear if it can be predictably controlled.

Bossi et al. [21] varied bond line thickness with steps from nominal (0.5 mm) up to 3 mm to achieve weak bonds. They also varied the number of laminate plies in pairings, including 10, 16, 20, 30, and 46, to evaluate the range of performance of bond line response.

2.1.5 Processing Variations—Clamping Pressure and Curing Temperature, Rate, and Time

Process variation papers were not as prevalent in the databases searched. However, experts in the field have suggested several options that could lead to the development of controlled weak bonds in metal substrates. Among those methods suggested are intentional exceedances of allowed out-times for the adhesive film materials and even partial pre-cures of the adhesives. However, it remains to be seen whether the bonds would be consistent across the entire bond line. It is possible that heterogeneous bond lines could be formed because of highly variable cross-linking across a bond surface.

2.1.6 Quality Control of Adhesive Bonding

Ensuring a full-strength durable bond requires a level of process control that is much higher than currently used in many other aviation structural maintenance repair activities. The materials and processes used for adhesive bonds are highly sensitive to a large number of factors; for instance, if maintenance technicians performing bond fabrication have not been properly trained, excessive variation in those factors can cause major degradations in bond strength without any apparent indicators. In fact, because of the complex chemistry and surface science involved, even trained technicians can commit errors that result in weak, nondurable bonds. It is essential that adequate engineering process controls be put in place and all requirements adhered to by fabrication personnel. To that end, AANC has developed a metal bond procedure, shown in appendix A, to support future work.

2.2 NDI FOR BOND STRENGTH

All NDI methods used for assessing the condition of materials or structures rely on a basic chemistry or physics principle. That is, each method revolves around a specific science that allows the interrogation of a material and the return of some indicator or signal that provides information on the condition of the material. In most cases, the indicator or signal is interpreted based on the similarity to another indicator or signal from a known real or simulated defect in a similar part or material to the one under test. For example, an eddy current signal is not actually detecting the presence of a crack. It is only measuring the increase in the inductive reactance of a coil in the inspection probe due to increases in the resistance to current flow when a crack is present. Typically, the crack will act as a resistor in the circuit and cause a change in the overall impedance. Because other factors can also cause similar changes to the circuit impedance, it is very important to have strong correlation between set-up signals from known defects and

indication signals from parts under inspection. Knowing the service history of the part can be equally important in making the final determination of the meaning of an indication signal. The main point is that most NDI methods use comparison of signals from parts under inspection to signals from parts with known defects. The greater the similarity between the two signals, the greater the likelihood of a defect being present in the part under inspection. Thus, a strong correlation exists between the eddy current signal and the presence of a crack, but there is no direct measurement of a parameter of the crack (e.g., crack length).

A good starting point for any review of nondestructive testing (NDT) methods used for adhesive bond assessment is the work of Hagemaier [27] in volume 17 of the ASM International Handbook. Hagemaier was one of the most active NDT practitioners in the commercial aerospace field for most of his career at Douglas Aircraft, later McDonnell Douglas. He presents a very practical, yet rigorous, engineering review of NDT as it was available for bond assessment up until roughly 1990. He presents information on several types of bond testing equipment and concludes that, although disbonds due to porosity, corrosion, and other gross defects are detectable, bond-strength measurement would require significant work. Fortunately, much progress has been made in the decades since Hagemaier's findings.

Of all the papers reviewed here, the most useful is the excellent summarization of NDT methods for bond-strength assessment provided by Ehrhart et al. [28]. The reader is encouraged to spend the time required to read this one paper before venturing into the large number of papers that have been written over the past 50 years. The brief summarizations Ehrhart et al. provide of the state-of-the-art for several major NDT methods are concise yet illuminating.

Caution is urged regarding accepting the conclusions of some authors because their supporting data are sometimes not presented or have been interpreted in the most optimistic manner possible. The preceding statement is made because the authors are not aware of any commercially available, portable, reliable, and affordable NDT equipment for bond-strength measurement. That being said, it is very clear that progress continues to be made in the development of bond-strength assessment tools and eventually one or more methods will be refined to the point of being commercially available and useful to the aircraft maintenance industry.

Adams [29] and Adams and Cawley [30] present an excellent comprehensive review of the common defect types and conventional NDT methods used to inspect composite bonded joints. The first part of these reviews consists of a brief introduction to the mechanical considerations of composites and adhesive joints, together with a description of the types of defects that may occur. The second part briefly describes the relevant conventional nondestructive techniques used in the late 1980s to identify these defects and indicates the sensitivity of each method to the different types of defect. Rose [31], Light and Kwun [32], and others also present incisive reviews of state-of-the-art NDI for bonded joints around 1990. Another important collection of papers were presented at the ASNT Fall Conference in 1989 [33]. The topical proceedings entitled "NDE of Adhesive Bonds and Bondlines," presents a compendium of papers by leading researchers at that time and very much supports the argument that there is no capability to measure bond strength directly from a conventional NDI method. Several papers, however, do support the use of advanced ultrasonic methods as having the potential to eventually provide bond-strength information. Bond quality assurance using local proof testing is also introduced as

a viable concept in these proceedings, as well as thermographic, acoustic, radiographic, optical, and holographic methods. To this day, though, even the most advanced bond-strength proof loading inspection equipment developed by Bossi et al. [21] requires a car-sized cart to move the inspection equipment to the airplane for use.

In the pure sense of bond-strength measurement, the degree of chemical bonding at the interface between adherends and adhesives determines the actual strength of the bond. Bardis and Kedward [34] present some advanced laboratory methods for inferring the degree of chemical bonding in an adhesive joint based on surface morphology or chemistry, but none of them is portable and useful in the industrial setting of a modern transport airplane maintenance hangar. Surface information is typically obtained from very small samples subjected to laboratory analytical methods, such as scanning electron microscopy for surface morphology, and energy dispersive spectroscopy, or x-ray photoelectron spectroscopy, for surface chemistry. All of these methods require the bonded specimen to be broken open to be analyzed. These examples are certainly not inspection methods useful for a large-scale repair panel on the side of a modern transport airplane sitting in a hangar or outside on the tarmac.

2.2.1 Criteria Defining a Promising NDI Method to Assess Adhesive Bond Strength

1. Method is applicable to all material systems:

    a. Composites
    b. Metals
    c. Hybrid composite/metals

2. Method is applicable to weak bonds arising from any factor or combination of factors.

3. Method can be implemented in industrial or manufacturing environment:

    a. Relatively quick inspection times
    b. Relatively affordable cost to acquire and implement
    c. Wide range of structures and applications can be assessed

4. Signal to noise ratio is high/ signal attenuation is low.

5. Directly measures or has statistical correlation coefficient of $R^2>0.9$ between NDI signal value and appropriate mechanical properties of the bond area (e.g., UT nonlinear parameter β, and fracture energy G_C):

    a. Shear load across a kissing bond
    b. Peel load
    c. Tension load
    d. Stiffness changes
    e. Fracture toughness changes

6. May need to induce stress in the part:

    a. Thermal stress
    b. Vibration/shear stress
    c. Mechanical stress
    d. Resonance/UT stresses

7. Method must be truly nondestructive.

2.2.2 Laser Shock Method—Localized Proof Loading

In two related papers, Russell [35 and 36] provides a short history of combined Air Force Research Laboratory (AFRL) and Boeing efforts to implement composites technology in United States Air Force (USAF) aircraft, including the rationale, goals, technology development, and assessment of bonded joint efforts. Summary results were presented from an AFRL $152 million, 11-year effort to address relevant issues. There was no mention of weak bond fabrication efforts, but the development for a laser shock method for bond-strength assessment was discussed. Also mentioned was the laser shock proof loading method (also called laser bond testing) commercialization effort by LSP Technologies Inc. The paper highlights that the USAF had led a large effort to address many issues of using composites in aerospace with some success. But it also points out that much work remains to be done, particularly in the area of repairing and inspecting composite laminate aerospace structures.

Bossi et al. [21 and 37] discuss adhesive bond strength in the plastic region of the stress/strain curve. They state that NDI must be done in the elastic regime of materials. The theory of bond mechanics is reviewed as it applies to the particular NDI method under investigation. To inspect the bond in the elastic region, they apply a tension load on the bond. A weak bond below a given strength threshold will fail. A laser is focused on a small spot to create an ultrasonic shock wave. The energy of the laser is easily adjusted, thus the failure threshold energy can be established. The authors used lap shear specimens of laminate CFRP bonded with industry standard adhesives. The laser bond inspection (LBI) method commercialized by LSP Technologies Inc. had good correlation between mechanical strength and laser shock measured strength. The authors are applying the concept that a level of stress that does not break the part has no short-term durability effects, even though some inspections might cause small disbonds. Long-term durability effects after repeated inspections are not discussed. Follow-on work has led to the development of realistic composite laminate weak bond specimens.

Perton et al. [24] also published work on evaluating the laser shock method for bond-strength evaluation. Laser shock waves induce high-amplitude ultrasonic wave propagation, which is measured by laser ultrasonic inspection. It is shown to be an adequate means of performing a proof loading method of bond quality assessment up to the failure threshold energy. Experimental results confirmed by numerical simulations show that the proposed method is able to differentiate weak bonds from strong bonds in composite laminate bonded structures and to estimate the bond strength quantitatively. It was shown that the shock waves propagate only under the elastic regime, and, when damage is the result of high strain rate deformation, the material exhibits brittle behavior. Thus, the method is useful as a non-invasive proof test that allows the strength measurement to be made quantitatively. Although the authors have done

significant work to develop the theoretical basis for quantitative bond-strength measurement, significant work remains before this method can be fielded in a maintenance environment because of the large amount of specialized specimen preparation and equipment required. That being said, the fundamental theory is sound for eventually developing a bond-strength measurement technique.

Finally, in recent work done in Europe, Ecault et al. [22] have developed a laser adhesion test system using the laser shock method similar to that developed by Bossi et al. [21]. Significant testing of the system has demonstrated the ability to discriminate different levels of adhesion in the case of weak bonds on CFRP laminates. Contamination of surfaces with mold release was effective in generating controlled weak bonds for system development and testing. Correlation between laser shock results and mechanical strength G_{IC} values was validated with post-mortem characterization by interferometric confocal microscopy, ultrasound inspection, and cross section direct observations of specimens.

2.2.3 Ultrasonic Methods

As early as 1960, researchers were investigating bond-strength measurements using ultrasonic methods. Frank and Schmitz [38] found that "preliminary tests on a number of adhesive bonds subjected to tensile stresses indicate that detection of the acoustic energy emitted by the bonds at frequencies about 16 kilocycles per second can be used as a method for determining bond strength." The authors used a piezoelectric transducer to detect acoustic energy generated by the adhesive bond as it is subjected to an increasing tensile stress. This method was found to be useful in measuring adhesive bond strengths on metal honeycomb core panels, but it had very limited success with phenolic cores, which introduce noise masking the acoustic signals generated by the adhesive bond.

Rokhin, Hefets, and Rosen [39] found that the phase velocity of the interface wave and the effective shear modulus of the interface film, calculated from the velocity data, are related to the strength of the adhesive bonds. The general transmission loss factor, a function of the relaxation maximum of losses arising during the course of polymerization of the adhesive, was another parameter correlated with the strength. Hodges, Tyeryar, and Berry [40] made bonded single-overlap shear specimens fabricated from Graphite/PEEK (polyetheretherketone) composite adherends and titanium adherends. The specimens were bonded by an electromagnetic induction technique producing high heating rates and high-strength bonds in a few minutes. Nondestructive evaluation of bonded specimens was performed ultrasonically by energizing the entire thickness of the material through the bond line and measuring acoustic impedance parameters. The authors claim that destructive testing confirmed the unique ultrasonic profiles of strong and weak bonds, thus establishing a standard for predicting relative bond strength in subsequent specimens. However, such acoustic impedance parameters have not been put into practical use.

Acousto-ultrasonic nondestructive evaluation of the adhesive bond strength between rubber and steel plates using the stress wave factor (SWF) measurement technique was investigated by dos Reis and Krautz [41]. They observed that higher values of the SWF measurements correspond to higher values of peel strength test data. The results show that the SWF technique has the potential to be used in adhesive bond-strength measurements.

In 1989, Smith and Yang [42] at NASA used the quadrature phase detection technique to simultaneously monitor the phase and amplitude of a tone burst signal normally reflected from an adhesively bonded steel-to-rubber interface. The measured phase was found to show a positive shift for all bonded samples with respect to the disbonded state — the phase shift being larger for samples with weaker bonds, as manifested by smaller values of applied tensile loads at failure. A model calculation, which incorporates the concept of interfacial strength into the usual problem of wave propagation in multilayered media, was used to deduce a bond-quality parameter from an experimentally measured phase shift. This bond-quality parameter was found to be correlated with the tensile strength of the adhesive bonds at failure loads. This method had apparently benefited from the use of a rubber adherend on one side because it had not been transferred to a structure with two rigid adherends.

In related work, Mal et al. [43] studied the role of the interface zones in the fracture and failure of bonded composite materials. The existing NDE methods at that time were generally not capable of yielding useful quantitative information on the strength of an interface. However, developments in ultrasonic techniques yielded very accurate estimates of the thickness and elastic moduli of adhesively bonded joints using guided waves launched in a direction parallel to the bonded surfaces. Certain properties of these waves are strongly affected by the interface properties. They carried out coordinated theoretical and experimental research and determined the nature of the relationship between the interfacial properties and the measurable properties of the guided waves. They demonstrated that a careful analysis of guided wave data can give highly accurate estimates of some of the interface properties in a variety of bonded systems.

Chance [44] developed weak adhesive bond specimens by fabricating with contaminated surfaces. He then used ultrasonic resonance methods to inspect the parts. The results indicate that the UT resonance technique was 97% effective in detecting weak bonds as determined through destructive test correlations but suffered false reject errors ranging from 14% to 31%. Difficulties were encountered with the destructive test correlations because of the wide variation of bond-strength results experienced with the flatwise tension tests that were conducted.

Lih [45] studied thermal degradation of adhesive bonds, both experimentally and through calculations. Aluminum and titanium lap joint specimens were used. Each was heated at 220° F for 1 hour. Leaky Lamb waves (LLW) dispersion curves were analyzed. The LLW phenomenon is induced when a pitch-catch ultrasonic setup insonifies a plate-like solid immersed in fluid. This phenomenon was discovered by Bar-Cohen et al. [46] while testing a composite laminate using a Schlieren imaging system. The phenomenon is associated with the resonant excitation of plate waves that leak energy into the coupling fluid and interfere with the specular reflection of the incident waves. The destructive interference between the leaky waves and the specularly reflected waves modifies the reflected spectrum, introducing a series of minima in the spectra of the reflected waves. The LLW experiment for composite laminate specimens involves measurement of the reflected field and extraction of the minima in the reflected spectra at various angles of incidence and orientations (polar angles) with respect to the laminate. The data are presented in the form of dispersion curves showing the phase velocity (calculated from Snell's law and the angle of incidence) of the LLW as a function of frequency. The sensitivity of the dispersion curves to variations in the properties of the composite material,

namely its anisotropy, layer thickness, stiffness constants, and the presence of defects, has made this phenomenon an attractive NDE method. Results show that there is a significant difference in the dispersion curves for heat damaged vs. undamaged specimens.

Rose et al. [47] developed an early bond-detection device using ultrasonic LLW and demonstrated it at the AANC in 1994. Gross disbond detection due to corrosion in aluminum lap joints and delamination in bonded tear strap doublers was effective and quick. The utility of guided waves for the investigation of adhesive bonds is reviewed in this paper.

Brotherhood et al. [48] investigated the effect of compression loading on detection of kissing bonds in aluminum coupons by longitudinal ultrasonic waves. They found that the detectability of kissing bonds depends upon a number of factors, including surface roughness, load, load history, adhesive properties, grease-adhesive system, and the degree of contamination used in fabricating the artificial defect. In general, increasing compression on a specimen decreases detectability by UT methods. In follow-on work published 2 years later, Brotherhood et al. [49] concluded that longitudinal wave, shear wave, and high-power ultrasonic inspection on dry contact kissing bonds were susceptible to contact pressure of the probe. Increasing contact pressure decreased sensitivity rapidly, with longitudinal waves having the greatest contrast at high contact pressures.

Adhesives exhibit linear stress/strain behavior until the onset of failure is indicated by a change in the material nonlinearity. Hirsekorn [25] describes in detail how binding forces are nonlinear and cause a nonlinear modulation of transmitted and reflected ultrasonic waves. Because of the nonlinear modulation, the generated higher harmonics can be used to distinguish between strong and weak bonds. Theoretical fundamentals are presented, including extensive calculations that describe how bond strength is obtained from data. However, limitations of the method exist because noise signals are often larger than higher order harmonic signals of interest and can be difficult to separate.

Qu [50] observed higher harmonics of the fundamental frequency generated when an ultrasonic wave passed through a nonlinear material. Results from numerical simulation show that material nonlinearity generates higher order harmonics. In particular, the elastic-perfect plastic material behavior generates significant 3rd and 5th harmonics. Qu discusses the work of several other researchers (Nagy et al. [51], Achenbach and Parikh [52], Parikh and Achenbach [53], Hirose and Kitahara [54], Anastasi and Roberts [55], Pangraz and Arnold [56], Tang et al. [57], Berndt and Green [58 and 59], Lowe and Cawley [60], Rose et al. [47], and Rose et al. [61]) who have developed theories/models supporting the nonlinear effect, and suggests that this nonlinearity can be effectively used to characterize bond strength. In this study, he used the ultrasonic parameter to characterize the “curing” state of a polymer/aluminum adhesive joint. Ultrasonic through-transmission was conducted on samples cured under various conditions. The magnitude of the second-order harmonic was measured and the corresponding ultrasonic nonlinear parameter was evaluated. Results indicate that the nonlinear parameter might be used as a good indicator of the cure state for adhesive joints, which would indicate one form of weakness in an adhesive bond.

Cantrell [62] discusses the fundamentals of nonlinear ultrasonic methods, including the development of nonlinear parameters. He cites Zheng et al. [63] as the source of the concept that

material nonlinearity parameters can be assessed because of resonant frequency shifts caused by variation of the amplitude of superposed continuous waveforms. Zheng states, "The experimental acoustic methods for the higher order elastic constants measurements have been demonstrated to be useful for the nondestructive evaluation of various disruptions in solid materials, like dislocations in crystals, fractions of precipitates in metallic alloys, microcracks, disbonds and other defects." In particular, the nonlinear coefficients β_n of the higher order terms in the local speed variation of an acoustic wave with particle velocity (or strain) "unambiguously provide a strong correlation" with the growth of such defects as strength degradation. Both of the previously mentioned references provide extensive reviews of prior work and should be of great value in understanding the fundamental physics of nonlinear methods. Acoustoelastic measurements take maximum advantage of sensitivity enhancements in continuous wave techniques. The sensitivity enhancements are due to the superposition of waveforms reflected from the bounding surfaces. Nonlinear methods have been shown to detect variation in sound velocity as a function of the state of stress of the material. Higher order elastic constants are measured as well as subtle changes in microstructure in metallic materials based on changes in acoustoelasticity. Thus, nonlinear parameters are thought by many to offer some potential for bond-strength assessment, with acoustoelastic measurements being of optimum interest. In fact, Heyman and Lynch [64] filed a U.S. patent for just such a device. From the patent application comes the following: "The invention is a measurement system comprised of an ultrasonic system (including a phaselocker), a stressing system, and a controlling/data processing system. The systems, methods, and apparatuses of this invention measure changes in the nonlinear anelastic material properties of the bond material using ultra-sensitive acoustic phase-locking propagation coupled to a controlled state-change, such as stress. Bond strength is determined from statistical comparisons with similar geometry sample tests characterized with this technique and subsequently loaded to failure." However, the success of the device is still unproven because there is, to date, no validation performed of the method. In fact, no validation capabilities even exist for determining the validity of claims pertaining to adhesive bond-strength measurements.

In Yan et al., the authors discuss the characteristics of kissing bonds and their investigation of ultrasonic inspection as a means to measure nonlinearity [65 and 66]. To accomplish this work, they made simple kissing bond samples (disbonds), but only one of each kind, using room temperature cure two-part epoxy. Perfectly bonded, fracture surface kissing bond, and contamination layer kissing bonds were made. The approach was to use a high-frequency through-transmission technique and measure the nonlinearity of the kissing bond from the distortion of the received signal under low-level compressive loading. Nonlinearity decreases rapidly with compressive load. A nonlinear parameter β' was defined as the ratio of the 2^{nd} harmonic divided by the square of the fundamental frequency (the input signal frequency). The experimental results from the fracture surface specimen showed that its nonlinear parameter was higher than the reference and was significantly affected by contact pressure, suggesting that the measurement of nonlinearity is a reliable technique for detection of fracture surface kissing disbonds at low loading levels. Yan et al. could detect low levels of contamination but had very limited data on only three specimens. Also, through-transmission ultrasonic inspection is not readily field deployable on airplanes and typically requires an elaborate squirter system that can inspect only components removed from the airplane. In 2012, the work of Yan et al. [67] concluded that, with the use of a one-dimensional time domain model, which includes an

interfacial nonlinearity to predict the interaction of ultrasonic pulses with a kissing bond model, the measured nonlinearity is highly dependent on the thickness of the adhesive layer-to-wavelength ratio. Overall, their work suggests that variations in the nonlinear parameter β' are due to changes in adhesive geometry and can be significant. Thus, using β' to quantify the adhesive joint condition is valid when a geometrically and materially identical, defect-free reference is available, or in comparison with modeled data.

In a large 1999 study funded by NASA, Achenbach and Tang [1] used external static tensile loading and a superimposed longitudinal wave to obtain the slopes of the stress-strain curve of an adhesive bond at a series of load levels. The critical load at which a reduction of the slope is detected by the superimposed longitudinal wave was an indication of the onset of nonlinear behavior of the adhesive bond and, therefore, of bond degradation. This approach was applied to the detection of adhesive bond degradation induced by cyclic fatigue loading. Analogously to the longitudinal wave case, a superimposed shear wave was used to obtain the effective shear modulus of adhesive layers at different shear load levels. The onset of the nonlinear behavior of the adhesive bond under shear loading was detected by the use of a superimposed shear wave. The experiments showed that a longitudinal wave can also detect the nonlinear behavior when an adhesive bond is subjected to shear loading. An optimal combination of UT and mechanical-loading methods for the detection of degradation-related nonlinear behavior of adhesive bonds was presented. For the purpose of a practical application, an ultrasonic technique using a temperature increase as an alternative to static loading was also investigated. A general strain–temperature correspondence principle that relates a mechanical strain to a temperature was presented. Explicit strain–temperature correspondence relations for both the tension and shear cases were derived. An important parameter that quantifies the relationship between the wave velocity and temperature was defined. This parameter, which is indicative of adhesive bond nonlinearity and which can be conveniently obtained by an ultrasonic measurement, was used as an indication of adhesive bond degradation. Experimental results showed that the temperature increase method was a convenient and productive alternative to static loading.

Yang. et al. [23] used UT damping loss factors and frequency measurements to monitor defects in composite joints, including weak bonds due to poor surface preparation. They found that the damping loss factors and frequency monitoring were somewhat effective in detecting damage or degradation of the bonded joint, but the overall results were variable.

Marty et al. [2] used ultrasonic resonance methods to detect kissing bonds in aluminum bonded samples with manufactured weak/kissing bonds. Results were promising and showed a reduction in shear wave resonance associated with weak kissing bonds.

Jian et al. [68] measured interface reflection ultrasonic waveforms using a spherically focused transducer. The results were explained using an interface spring model for a small spot size rather than for an average large area. The UT waveforms and C-scan images showed correlation with shear stress measurements and thermal cycling history. This higher degree of correlation is not seen in other UT studies, probably because of the higher uniformity of the specimens and the small spot size of the UT beam. However, the paper generally supports using UT for bond-strength measurement in certain situations.

Stratoudaki et al. [69] have developed a noncontact ultrasonic transducer system (CHOT), which is optically excited by means of lasers and can be used for both UT signal generation and detection. The development was demonstrated using surface acoustic waves but can be adapted to any UT method. According to the authors, optical transducers have improved sensitivity in nonlinear UT. Nonlinear UT examines certain harmonic responses and is one UT technology that still may have potential bond-strength assessment capability. The authors claim increased sensitivity to material microstructural changes and high signal-to-noise ratios, which may allow for detecting harmonic changes that could be correlated to bond strength.

Roach et al. [14] presents results from a program with the three major U.S. auto manufacturers to use NDI to map the placement and thickness of adhesives in auto body components and to measure bond strength. Various contaminants were used to make weak bond metal-to-metal specimens. Several different NDI methods were employed, most of them based on linear UT. Results of inspections show that adhesive placement and thickness are determined, but they were inconclusive with respect to measuring bond strength. The most promising results of bond-strength measurements were based on a linear UT method that is similar to laser shock methods in that threshold failure strength was possibly measured.

Klein [70] applied a laser ultrasonic inspection system for use in the auto manufacturing industry. Samples provided by Roach et al. [14] supported system development and validation. Techniques were developed to map the adhesive spread and measure the adhesive thickness. The signal processing efforts indicated a pathway for processing the raw data in real time and defined a pathway for measuring the adhesive bond strength. This involved examining the ratios of magnitudes of adjacent interface-echo arrivals when moving the laser beams across the sample. A general trend of decreasing later arrivals with increasing bond strength for most of the samples was observed when comparing time-traces from samples with different bond strengths.

Nagy and Adler [71] laid a solid foundation in 1989 for bond-strength assessments using leaky guided interface waves to inspect aluminum plates bonded with FM300 adhesive. Both theoretical and experimental means were employed to show that conventional Lamb wave inspection of adhesive joints is mainly sensitive to the properties of the adherend plates and much less to those of the adhesive layer and the crucial interface between them. Because of weak acoustical coupling through the adhesive layer, only the amplitudes of certain Lamb modes, but not their frequencies, are strongly affected by bond defects. However, guided interface waves are more sensitive to both adhesive- and cohesive-type defects and are much easier to interpret and evaluate. In 1991, Nagy, McGowan, and Adler [51] discussed the strengths inherent to nonlinear ultrasonic methods for assessing bonds.

In a 2012 proposal to the FAA for developing a diffusion bond-strength-assessment method, Nagy [72] discussed the reason that nonlinear UT has not found wider acceptance for bond-strength measurement: "The main reason is that the most sensitive nonlinear harmonics generation techniques are also very sensitive to spurious nonlinearities that inherently arise in the driving electronics, transducers, and, especially, in the coupling medium between the transducers and the component to be inspected. These spurious nonlinearities could be comparable, or even stronger, than the combined intrinsic material nonlinearity and excess nonlinearity caused by material imperfections." He has proposed the development of a nonlinear UT imaging method,

termed non-collinear mixing, that removes the unwanted signals and allows distinction between higher order harmonics of material with and without imperfections. According to Nagy, this approach was first proposed by Jones and Kobett [73], experimentally observed by Rollins [74], and then further developed by several other researchers. Nagy states, "Non-collinear mixing exploits the fact that material nonlinearities cause interaction between two intersecting ultrasonic waves. Under certain circumstances, this can lead to the generation of a third wave with a frequency and wave vector equal to the sum of the incident frequencies and wave vectors, respectively. By measuring the magnitude of the mixed harmonic, the degree of material nonlinearity can be quantified." While the method is being proposed for determining bond strength in diffusion bonded jet engine metals, the theory is also applicable to adhesive bonds between aluminum and composites.

In some of the most recent work reviewed, Vijaya Kumar et al. [75] performed experimental and theoretical studies on degradation measurement using oblique incidence UT on CFRP substrates bonded with epoxy adhesive. Weak bonds were fabricated by adding varying amounts of poly vinyl alcohol (release agent) to the adhesive, which creates porosity. Adhesive degradation was detected as significant variation in reflection amplitude and also by a shift in the minima of reflection spectrum. It was observed that severe degradation of the adhesive leads to adhesive failure mode. This study demonstrated a correlation between bond strength and a frequency shift in reflection minimum. However, validation of experimental data was performed using analytical models only. The authors state that more progress can be made by creating more specimens with different amounts of interfacial degradation while maintaining bulk adhesive properties.

2.2.4 Thermography Methods

In a Polymer Science USSR paper, Zaitsev [76] discusses the fracture activation energies of normal and weak adhesive bonds in terms of theoretical calculations. He shows that fracture activation energy varies with bond strength and should be less for weak bonds (those bonds with damaged polymer links). While the calculations show only small activation energy changes occur between normal bonds and weak bonds during fracture, they do indicate a direct relationship between the degree of polymer bonding and temperature generation under stress. Stress in bonds can be generated by a number of methods, including mechanical, thermal, optical, and ultrasonic. Because infrared (IR) emissions are related to temperature changes raised to the 4^{th} power, it is feasible that IR can be used to detect even small temperature differences between strong versus weak bonds during ultrasonic excitation.

Rantala, Wu, and Busse [77] discuss the use of amplitude-modulated lock-in vibrothermography for NDE of polymers and composites. The method uses mechanical heat excitation with generated stresses converting mechanical energy into thermal energy due to acoustical damping. Magnitude and phase of the sample temperature with respect to the modulation are measured with the IR camera and software lock-in technique. The use of thermal phase information increases the reliability of the defect detection and the application of high vibration frequencies provides good thermal signals at low stress levels. The researchers reported detection of impact damages, inclusions, voids, cracks, paint thickness, and, most importantly, evaluation of stress-level distributions and quality of bonding. Three phenomena are cited as being beneficial for the use of vibrothermography as a method for elucidating bond strength. These phenomena are the

strong acoustical damping of polymers, which causes good heating at low stress levels; high IR emissivity of polymers; and low thermal conductivity of polymers, which keeps generated heat localized to defect areas.

Meola et al. [78] used both pulsed and lock-in thermography to examine the effects of various defects on direct (time/temperature) and phase images from IR cameras. The lock-in technique uses thermal waves instead of pulses and, thus, the phase image gives direct indications. Both optical (heating lamp) and ultrasound (elastic waves) lock-in thermography have the potential to provide information on bond quality. This study used only optical lock-in thermography but did measure variation in bond line thickness and adhesion improvements induced by surface modifications (abrasion) and type of adhesive. The authors feel that IR thermography is still not completely adopted as an NDE tool.

Genest et al. [79] proposed using pulsed thermography for the detection of disbond and the monitoring of disbond growth in bonded graphite repairs. The authors correlated results with ultrasonic pulse-echo C-scan inspections. Destructive testing showed good disbond detection capability with accuracy similar to that of ultrasonic inspection.

Renshaw et al. [80] discussed crack closure effects on heat generation in metals, but, more importantly, pointed out that heat generation can be modulated based on externally applied stresses. The closure state of a crack (which also applies to bond line cracking), the level of applied vibration, and externally applied stresses influence the regions of a crack that will generate heat. According to Holland [81], crack detectability and reliable and repeatable vibration generation in the specimen are major issues to be addressed for this method to be fully applicable in the aerospace industry. The amount of heat dissipated by a crack depends on dynamic strain in the vicinity of that crack. Probability of detection of a crack is high in the regions where the vibrational strain in the specimen is high, and it is reasonable to expect the same would be true for weak bonds. Hence, the ability to detect a crack (or a weak bond) using vibrothermography relies on applying sufficient dynamic strain to make the crack generate detectable amounts of heating. The implication is that an in-depth understanding is required to excite a bond to obtain desired responses and eventually determine bond strength. Another implication is that vibrothermography has strong potential to detect disbonds that have already occurred and, with careful selection of testing parameters, has some potential to provide information about bond strength based on degree of cross-linking both within the adhesive layer and, especially, at the adherend/adhesive interface.

Sathish et al. [82] present a noncontact acousto-thermal signature (NCATS) nondestructive evaluation technique. The physical basis for the method is the measurement of the efficiency of the material to convert acoustic energy into heat. The increase in temperature due to conversion of acoustic energy injected into the material without direct contact was found to be dependent on the thermal and elastic properties of the material, both of which can be related to the degree of polymer bonding. The potential of the NCATS technique to detect microstructural-level changes in materials, such as degree of cross linking at bond interfaces and within adhesive materials, was demonstrated by evaluating accumulated damage due to plasticity in Ti-6Al-4V and low-level thermal damage in polymer matrix composites.

It is reasonable to conclude that thermography coupled with the proper form of excitation shows a strong potential for further development into a bond-strength measuring or correlating method. Additionally, the IR camera technology advances of recent years and the reduction in cost of high-end research cameras support this conclusion.

2.2.5 Shearography Methods

Shearography or speckle-pattern shearing interferometry is a measuring and testing method similar to holographic interferometry. Coherent light or sound waves are used to provide information about the quality of different materials in NDI, strain measurement, and vibration analysis. Holographic interferometry enables static and dynamic displacements of objects with optically rough surfaces to be measured with very high precision (fractions of a wavelength of light). Fringes can be obtained by making two recordings of the light field scattered from the object on the same recording medium. The reconstructed light fields may then interfere, causing fringes to form, which map out the displacement of the surface. Measurements of displacement can be applied to stress, strain, and vibration analysis as well as NDI. If weak bonds allow more deformation than full-strength bonds, these methods are theoretically capable of measuring such deformation. However, full development of the method is still in process to this day, with companies using various methods to induce small amounts of stress into the part and some form of holography to measure strain displacements. The rapid transition of adhesive bonds from linear to nonlinear stress/strain behavior just prior to failure complicates the use of these methods.

Myers [83] reported that laser interferometry (electronic shearography) was the technically superior method—among a wide array of methods tested—for detecting debonds in solid rocket-booster thermal-protection systems. Methods included IR thermography, radiography (e.g., computed tomography), acousto-ultrasonics, mechanical/acoustic impedance, ultrasonics, acoustic emission, and the tap test. Capabilities, advantages, disadvantages, and relative performances in defect detection of each test method for bonding applications were reported.

Shankar and Fei [84] developed a conceptual model for the analysis of peel behavior of weakly bonded adhesive joints. The work focused on modeling weakness in adhesion caused by deterioration of the adhesive bond line, as opposed to weakness in cohesion. The degradation of the bond line interface in a weak joint was modeled by considering reduced properties for the bond line interface. Finite element analysis of bonded doubler joints and double lap joints was carried out to study the peel deformation on the surface of the outer adherends. It was shown that when a doubler or a double lap joint has a good bond on one side and a weak one on the other, the reduction in the strength of the bond line on the weak side causes an asymmetric distribution of the load transferred by the outer adherends, resulting in bending. The bending deformation accentuates the peel deformation on one side while diminishing that on the other, resulting in a considerable difference in the distribution of out-of-plane displacements on the two sides. Measurement of the differences in the distribution of out-of-plane displacements using sensitive optical methods, such as holographic interferometry, could, in theory, enable the detection of weak adhesive bonds by NDI.

Heslehurst [85] used holographic interferometry to inspect adhesively bonded joints with and without discontinuities. The characteristics of the holographic interferometry output and

relationship of the output to the bonded joint structural behavior showed that a few characteristics of the fringe pattern can be used to identify weak bond lines. Fringe pattern variation was observed over anomalous bond line regions. Loads required to produce weak bond fringe pattern variations were significantly different between weak bonds and disbonds. Although the initial work showed promise for determining bond strength nondestructively, a portable system capable of being used in a maintenance environment has not been developed. It should be noted that this method is not a direct measure of bond strength and requires correlation of obtained signals to actual bond strengths.

2.2.6 Other Methods

Other NDI methods for bond-strength measurement have been proposed by various authors but have received little attention in the literature. They include:

1. Hewitt [86] researched nuclear quadrupole resonance for bond inspection in the late 1960s and early 1970s at the NASA Marshall Space Flight Center. The technique is very sensitive to the nature and symmetry of the bonding around the nucleus of atoms in the material under test. Shifts in the quadrupole moment can be related to degree of bond and, theoretically, to bond strength. However, this application depends on adding cuprous oxide to the adhesive prior to bonding. It also requires that the structural materials being bonded are RF-transparent between the adhesive and the resonance probe. Thus, the method is not possible in aluminum structures because it is opaque to the RF excitation energy. This method requires substantial laboratory equipment and modified adhesives that, from a practical standpoint, prevent implementation in a field or hangar environment.

2. In a simplification of the work with laser shock bond testing, Yang et al. [13] used impact testing combined with electromagnetic acoustic transducer sensors to detect kissing bonds but did not evaluate the method for strength measurement. They were successful in detecting disbonds and kissing bonds, but it is not likely that users will want to perform gross impacts on newly installed repairs as required by the method.

3. Thermoelastic stress analysis (TSA) is discussed in detail by Greene et al. [87]. In general, TSA is a relatively simple method for surface stress measurement that yields the change in the sum of the principal surface stresses during a loading event. The method uses a focal-plane array IR camera to measure small changes in surface temperature with changes in loading. In this sense, it is essentially another form of shearography. Some of the advantages are that it provides full field, noncontact stress information with a resolution similar to strain gauges and it has high spatial resolution. A wide range of materials and structures can be analyzed over a broad frequency range with little setup or specimen preparation.

4. Abou-Khousa et al. [88] performed a comparative study of the capability of x-ray computed tomography, millimeter wave, shearography, and through-transmission ultrasonic methods for inspection of honeycomb composites. Two honeycomb composite panels were produced with several embedded flaws and missing material, primarily representing planar disbonds at various levels within the thickness of the panels and

possessing different shapes. Results of inspections of both panels with each method were compared and various strengths and weaknesses were shown for each. In general, x-ray CT had the highest defect detection rate and resolution, with near-field millimeter wave being next. However, no clear frontrunner method was observed for all defect conditions or in consideration of such factors as inspection speed, cost, lateral resolution, depth of penetration, and ability to resolve multiple overlapping defects.

5. Pethrick et al. [89] developed a dielectric spectroscopy method of nondestructively assessing the moisture content and structural integrity of adhesively bonded joints. Joints made of CFRP adherends bonded with AF 163-2K were aged and inspected with high- and low-frequency measurements. Dielectric behavior was studied in both the frequency and the time domains. Frequency domain analysis allowed the amount and effects of moisture ingress in the bond line to be assessed. Time domain analysis highlighted the onset of joint defects with increasing exposure time. Mechanical testing of the joints was carried out to enable correlation between changes in strength and failure mechanism due to moisture ingress, with changes in the dielectric data.

   In related work, Davis et al. [90] made aluminum-to-aluminum, aluminum-to-composite, and composite-to-composite bonded specimens and exposed them to hot wet conditions while taking electrochemical impedance spectroscopy (EIS) spectra across the entire bonded assembly. Periodic mechanical tests were conducted to obtain bond-strength values as a function of exposure. The low-frequency impedance correlated with bond strength of the humidity-exposed specimens and showed the same Arrhenius dependence, suggesting that moisture absorption by the adhesive was the limiting factor in bond performance and that EIS has the potential to nondestructively track bond health and warn of deterioration.

2.3 SPECIMEN BOND-STRENGTH TESTING METHODS

Anderson et al. [91] and Pocius [92] present engineering methods used to perform analysis and testing of adhesive bonds. These fundamental textbooks discuss the mechanical properties of materials as they relate to adhesion. Strain energy density is discussed as it relates to crack initiation, and linear elastic fracture mechanics are presented as they relate to crack extension, for which the critical strain energy release rate must be exceeded for the crack to propagate. The discussions highlight one of the fundamental issues associated with measuring bond strength nondestructively, which is that the energetic relationships in adhesive bonds prior to bond failure are a combination of Hookean solids and Newtonian fluids. Hookean materials store energy and return it during each loading cycle, while Newtonian fluids dissipate energy with each cycle. Polymer adhesives properties are somewhere in-between that of Hookean solids and Newtonian fluids. Their behavior is complex. Measuring changes of internal energy with applied stress are not topics that have been traditionally addressed by NDI methods. NDI typically measures change in a particular physical property. However, because the loading and unloading curves lie on top of each other, there is no observable change in the physical structures with viscoelastic adhesive bonds, which would indicate a reduction in the load carrying capacity of the bond. Any method that is capable of nondestructively determining load-carrying capacity of an adhesive bond must be capable of deriving the internal energy state of the bond, either by direct measurement or by correlation to some other physical property.

Mechanical strength and failure mode are the two main issues that arise when considering bonded joints. Mechanical strength can be measured by several destructive methods, depending on the particular failure mode of interest. All strength measurements are embodied as American Society for Testing and Materials (ASTM) standardized test methods. Test standards commonly used, the loading applied to the adhesive bond, and the failure modes are:

- Tension loading—Wedge test, ASTM-D 3762-98 Standard Test Method for Adhesive-Bonded Surface Durability of Aluminum; often combined with environmental conditioning, such as hot/humid exposure.

- Shear loading—Lap shear tests, ASTM-D 3165-07, Standard Test Method for Strength Properties of Adhesives in Shear by Tension Loading of Single-Lap-Joint Laminated Assemblies; ASTM-D 5868-01 Standard Test Method for Lap Shear Adhesion for FRP Bonding; ASTM D-1002-01 Standard Test Method for Apparent Shear Strength of Single-Lap-Joint Adhesively Bonded Metal Specimens by Tension Loading (Metal-to-Metal); and ASTM-D 3528-96 (Reapproved 2002) Standard Test Method for Strength Properties of Double Lap Shear Adhesive Joints by Tension Loading (provides peel-free stress distribution for engineering strength values; all tests perform shear loading parallel to the bonded surfaces by applying tension to lap specimens).

- Cleavage loading—Double cantilever beam test, ASTM-D 1062-08 Standard Test Method for Cleavage Strength of Metal-to Metal Adhesive Bonds; cleavage loading of more ridged metal and composite specimens.

- Peel Loading—Peel Strength Test, ASTM-D 1781-98 (Reapproved 2012) Standard Test Method for Climbing Drum Peel for Adhesives; used when one bonded surface is flexible, the other is rigid, and peeling failure is a concern.

- Compression Loading—This loading mode is generally not a concern for aerospace applications.

Failure mode (figure 1) is determined by examination of mechanical strength specimens after failure. Adhesive failure is defined as failure at the adhesive/adherend interface. Cohesive failure is defined as failure within the adhesive layer while the adhesive/adherend interface remains intact. One line of reasoning places greater concern on adhesive failures than on cohesive failures. Failure within the adhesive layer is considered easily resolved by selecting a stronger adhesive that is addressed during initial bond design. Thus, cohesive failures are not expected and are of less concern. Adhesive failures are considered much more likely in service, so fabricating specimens exhibiting this failure mode is more desirable as a starting point for research. Ideally, though, any NDI method of bond-strength measurement would accommodate either failure mode because bond strength is more closely related to internal energies than failure mode.

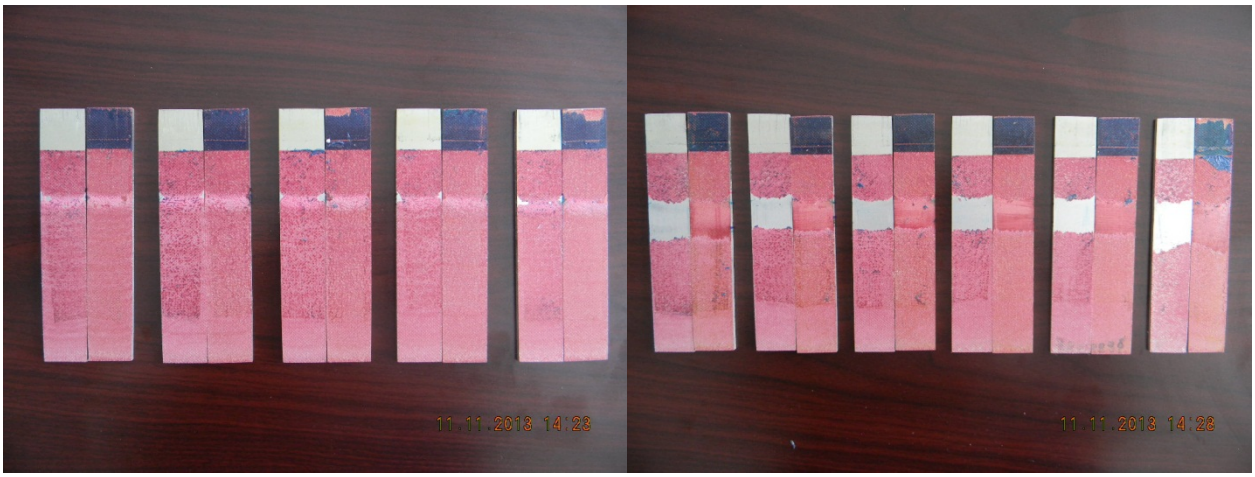

Figure 1. Examples of Wedge Test Specimens Showing Bond Failure Modes, With Cohesive Failure on the Left and Adhesive Failure on the Right

3. CONCLUSIONS AND RECOMMENDATIONS FOR FUTURE RESEARCH

3.1 WEAK BOND FABRICATION

Full development of NDT methods for bond-strength assessment depends on the availability of appropriate specimens to support development efforts. Currently, there is no national or international clearing house producing such samples. While the airplane manufacturers are conducting research on bonding, their work is proprietary and generally not available to all NDI equipment developers and vendors. While airplane manufacturers do provide development specimens for select NDI developers, proprietary information restrictions mean the results of NDI development efforts remain unshared. Limiting information sharing within the NDI industry generally slows the overall progress of developing and fielding new methods. One recommendation of this report is that the FAA support the development of weak bond specimen sets to be provided to the NDI community. Further, multiple fabrication methods must be developed, with each set designed to facilitate the fabrication of weak bonds for a given material system and structural configuration. The type of NDI method that could be developed and validated using a given specimen set will be dictated by the physics employed by the NDI and the interaction with the material and configuration.

Weak bonds with controlled strength and predictable failure modes can be made, but this first requires establishing a well-controlled fabrication process. Using statistical process-control variables, such as wedge test crack length, lap shear tension failure loads, bond line thickness, and bond failure mode will provide understanding of critical process parameters and eventual definition of a process with a high degree of control. Maximizing control of the process is the first critical step in fabricating adhesive bonds with tailored strength and desired failure mode.

The second step in the successful fabrication of weak bonds is deciding which defects are of prime importance and determining the failure modes caused by such defects. Clearly, adhesive mode failures are a concern because they indicate either a deficiency in the bonding process or

in-service degradation of the bond, both of which can lead to premature structural failure. While cohesive mode failures are of concern if they are caused by in-service degradation, it is still the case that an engineering design change in the adhesive used is the correct way to resolve the issue. With the large number of processing steps involved in bond fabrication, a very large array of experimental variables can be envisioned. However, the literature does have more weak bond fabrication work performed in the areas of surface preparation, contamination, bond line thickness, and certain processing variations. Specific recommendations for weak-bonding fabrication work are shown in table 1.

Recommendations for generating weak bonds on aluminum substrates with epoxy adhesives focus on surface preparation variations from a standard recipe for a full-strength bond. Building on the extensive work of others with variations in organosilane treatments to tailor bond strengths is suggested. Use of treatment variations that do not involve in-depth tailoring of chemical reactions is also recommended. Another suggestion is to use commercially available adhesives (either films or paste kits mixed on-site) in the same way that a repair facility would use them, and then expose them to overall processing variations that could occur in the actual maintenance environment. One notable excursion from a standard surface preparation step involves the natural aging of organosilane (Boe-Gel) beyond specified pot-life. Other surface treatments should also be explored using contact angle or other quantitative methods of determining the surface free energy of the substrate. Pretreatment methods that might yield high repeatability from fabrication run to run, as well as high uniformity across individual specimens, should be explored to their fullest.

Table 1. Experimental Matrix for Metallic Weak Bond Fabrication Research

Processing Step	Variables	Specific Parameters			
Surface Preparation on Airplane Panel	Low Humidity & Long Drying Times	RH<10% & Time >90 minutes			
	Aged Mixed Boe-Gel	0, 15, 30, & 45 days after mixing			
	Dilute Boe-Gel	1,3,9, & 15 (Si + Zr) Vol%			
	Eliminate Boe-Gel	0% Concentration			
	Substitute Alodine for Boe-Gel	IAW Alodine Application Requirements			
Surface Preparation on Repair Panel	Substitute Unapproved Primer for PAA	Spray on Primer, & Alodine			
	Dilute Primer	100, 75, 50, 25% Concentrations on PAA			
	Eliminate Primer	PAA surface only			
Contamination on Airplane or Repair Panel	Diluted Release Agent				
	Grease				
Bond Line Thickness	Add Extra Adhesive Film Layers	2, 3, 5, & 7 layers FM163-2 Film	Additional Parameters		
Processing - Partial Pre-Cures	Out Time, Out Temp., Out Rel. Humidity	30 & 60 min, 100 & 150 F, 50 & 95% RH	Time (min)	Temp (F)	RH (%)
			30	100	50
			60	150	95
Processing - Incomplete Cures	Ramp Rate, Cure Temp., Cure Time	1&3 F/min, 150 & 200F, 30 & 60 min	Ramp Rate	Temperture	Cure Time
			1	150	30
			3	200	60
Processing - Aged Adhesive Films	Months Beyond Expiration Date	6, 12, 18, 24 months			

PAA = Phosphoric acid anodization

3.2 NDI BOND-STRENGTH MEASUREMENT

Measuring the strength of an adhesive bond without loading it to failure is theoretically possible. The particular method will likely be based on fundamental physical properties of the materials involved correlated to strength values obtained through conventional strength testing. It is unlikely that any particular method will directly measure load-carrying capacity without actually applying a load. This paradigm is no different than that already used for most NDI methods inspecting for defects.

The laser bond testing method is leading the way regarding its ability to quantify bond strength in a nondestructive way. At least two other NDI methods show significant promise of eventually providing bond-strength measurements using NDI equipment common to the aerospace industry. These methods are nonlinear ultrasonics and noncontact vibrothermography. Shearography, whether it be heat or laser excited, has the ability to measure stress levels in the surface layers, but there is no current way to relate stress to bond strength in a practical way for individual and varying structural configurations, such as those found in repairs.

3.2.1 Laser Shock or Laser Bond Testing

Review of the literature indicates that one NDI method, laser shock testing (figure 2), has been developed to the point of being available to industry, although at a high cost. Additionally, laser shock testing only provides bond-strength information as a failure threshold or proof loading level. Structural engineers have been reluctant to accept this method because of the limitations of the data and also possibly because of the small amounts of damage that are imparted to bonds during testing. Equipment has been developed by separate organizations in both the United States and Europe. The technology readiness level (TRL) of the U.S.-based system is approximately 8–9.

Figure 2. Fieldable LBI Device [37]

3.2.2 Nonlinear Ultrasonics

The most advanced form of UT with significant promise of providing bond-strength information is non-collinear nonlinear UT. The cost of the equipment is projected to be relatively low compared to other advanced methods, and the developers plan to integrate the method into existing UT C-scan equipment. Nagy [72] states, "The main hurdle nonlinear c-scan imaging must overcome to become a practical inspection tool is the rejection of spurious coupling nonlinearity between the transducer(s) and the component to be inspected." In the case of immersion scanning, the coupling nonlinearity is due to the excessively high acoustic nonlinearity of the coupling fluid, usually water, relative to the modest intrinsic nonlinearity of metals and other structural materials. The intrinsic nonlinearity of the intact material is significantly increased in the presence of localized (e.g., interface) imperfections that cause excess nonlinearity, but this remains small relative to the huge coupling nonlinearity in liquids. Non-collinear mixing completely eliminates the adverse effects of both coupling and additional system nonlinearities. Currently, the method is performed in an immersion tank (figure 3); however, development of the method with another form of sound transfer—such as that used with conventional couplants—will be required to transfer the technique into an aviation maintenance hangar. The method is still in the developmental stages, with a TRL of approximately 5–6.

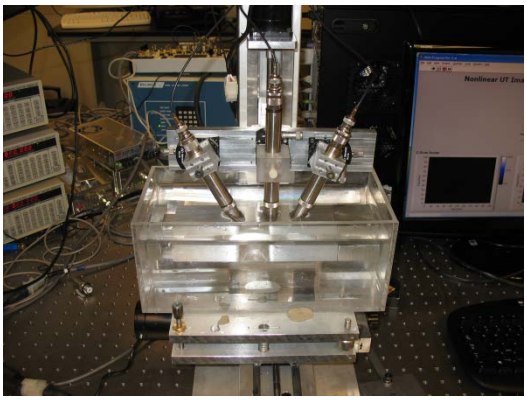

Figure 3. Immersion-Mode Non-Collinear Mixing Apparatus [72]

3.2.3 Noncontact Vibrothermography

Researchers at University of Dayton Research Institute have developed both the theoretical basis and initial equipment needed to implement noncontact vibrothermography (figure 4). Both thermal and elastic properties of the material form the physical basis of the system and are responsible for the conversion of acoustic energy to heat. The equipment consists of an ultrasonic horn that can produce high-amplitude waves (common in the plastic welding industry), a high sensitivity IR camera, and a computer. The plastic welding system and IR camera are both relatively high in cost, but advances in both of these fields have reduced the costs substantially from what they were just a few years ago. Further, the subtle temperature changes observed during research have demonstrated thermal damage in polymer matrix composites. However, like other NDI methods, heat signatures from bond interfaces must be correlated to known bond-strength standards through experimentation and theoretical modeling to gain quantitative bond-strength measurements. The TRL of this method is estimated to be between 4 and 6.

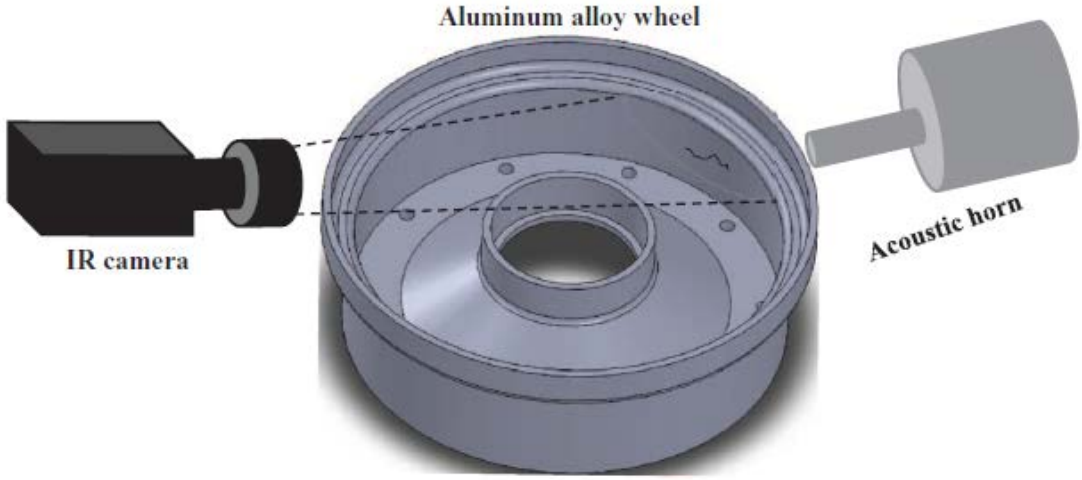

Figure 4. Position of the IR Camera, Acoustic Horn, and Wheel Component Under Inspection With Noncontact Vibrothermography [82]

4. REFERENCES

1. Achenback, J.D. and Tang, Z., "An Ultrasonic Technique to Determine the Residual Strength of Adhesive Bonds," Langley Research Center, NASA Technical Reports Server, Document ID: 20000034898, 2000, p. 142.

2. Marty, N.P., Desai, N., and Andersson, J., "NDT of Kissing Bond in Aeronautical Structures," 16th World Conference for NDT, Montreal, Canada, 2004, p. 8.

3. McCray, D., Smith, J., Mazza, J., and Storage, K., "Evaluation of Adhesive Bond Primers for Repair Bonding of Aluminum," *Presentation to 2011 DoD Joint Committee on Tactical Shelters*, 2011.

4. Lefebvre, D.R., Ahn, B.K., Dillard, D.A., and Dillard, J.G., "The Effect of Surface Treatments on Interfacial Fatigue Crack Initiation in Aluminum/Epoxy Bonds," *International Journal of Fracture* (Netherlands), Vol. 114, No. 2, 2002, pp. 191–202.

5. Tracey, A.C., Flinn, B.D., Blohowiak, K., Van Voast, P., and Grace, W., "Effect of Variables on Contact Angle Measurements for Peel Ply Composite Surfaces," SAMPE, Seattle, WA, 2010, p. 14.

6. Dillingham, G., Oakley, B., Van Voast, P.J., Shelley, P.H., Blakley, R.L., and Smith, C.B., "Quantitative Detection of Peel Ply Derived Contaminants via Wettability Measurements," *Journal of Adhesion Science and Technology*, Vol. 26., No. 10–11, 2012, pp. 1563–1571.

7. Liu, J., Chaudhury, M.K., Berry, D.H., Seebergh, J.E., Osborne, J.H., and Blohowiak, K.Y., "Effect of Processing Conditions on Adhesion Performance of a Sol-Gel Reinforced Epoxy/Aluminum Interface," *Journal of Adhesion Science and Technology*, Vol. 22, No. 10–11, 2008, pp. 1159–1180.

8. Abel, M.L., Allington, R.D., Digby, R.P., Shaw, S.J., Porritt, N., and Watts, J.F., "Understanding the Relationship Between Silane Application Conditions, Bond Durability and Locus of Failure," *International Journal of Adhesion and Adhesives*, Vol. 26, No. 1–2, 2006, pp. 2–15.

9. Abel, M.L., Adams, A.N.N., Kinloch, A.J., Shaw, S.J., and Watts, J.F., "The Effects of Surface Pretreatment on the Cyclic-Fatigue Characteristics of Bonded Aluminum-Alloy Joints," *International Journal of Adhesion and Adhesives*, Vol. 26, No. 1–2, 2006, pp. 50–61.

10. Underhill, P.R. and DuQuesnay, D.L., "The Dependence of the Fatigue Life of Adhesive Joints on Surface Preparation," *International Journal of Adhesion and Adhesives*, Vol. 26, No. 1–2, 2006, pp. 62–66.

11. Jeenjitkaew, C., Luklinska, Z., Guild, F., "Morphology and Surface Chemistry of Kissing Bonds in Adhesive Joints Produced by Using ElectRelease™ Adhesive," *The Journal of Adhesion*, Vol. 87, 2011, pp. 291–312.

12. Leclerc, J.S., "Weak Bond Characterization and Detection in Composite Structures," American Helicopter Society 65th Annual Forum, Grapevine, TX, 2009.

13. Yang, Y., Xiang, D., Qin, Y., Li, F., and Coulter, R.V., "Bond Inspection by Impact Test," Review of Quantitative Nondestructive Evaluation, Vol. 29, 2010, pp. 1206–1213.

14. Roach, D., Rackow, K., Nelson, C.L., Duval, R., and Moore, D., "Nondestructive Inspection of Adhesive Metal/Metal Bonds," DOE Final Report on USCAR NDI, 2010, pp. 10–1 to 10–11.

15. Underhill, P.R., Rider, A.N., and DuQuesnay, D.L., "The Effect of Warm Water Surface Treatments on the Fatigue Life in Shear of Aluminum Joints," *International Journal of Adhesion and Adhesives,* Vol. 26, No. 4, 2006, pp. 199–205.

16. Barroeta-Robles, J., Cole, R., and Sands, J.M., "Development of Controlled Adhesive Bond Strength for Assessment by Advanced Non-Destructive Inspection Techniques," SAMPE, Seattle, WA, 2010, p. 15

17. Biegert, L.L., Anderson, G.L., Evans, K.B., Olsen, B.D., Weber, B.L., and McCool, A.A., "Aging Effects of Environmentally-Friendly Cleaners on Adhesive Bond Integrity," Marshall Space Flight Center, NASA Technical Reports Server, Document ID: 20000105200, 2000.

18. Kinloch, A.J., and Kodokian, G.K.A., "The Adhesive Bonding of Thermoplastic Composites," Imperial College of Science and Technology, UK, 1989.

19. McDaniel, D., Zhou, X., and Pribanic, T., "Effect of Contamination on Composite Bond Integrity and Durability," Technical Review Presented to Joint Advanced Materials and Structures Center of Excellence, 2012, p. 22.

20. Chamochin, R., Cano de Santayana, M., Abenojar, J., Pantoja, M., Ballesteros, Y., and del Real, J.C., "The Effect of Surface Treatment on the Behavior of Toughened Acrylic Adhesive/GRP (Epoxy) Composite Joints," *Journal of Adhesion Science and Technology*, Vol. 24, No. 11–12, 2010, pp. 1903–1916.

21. Bossi, R., Housen K., Walters, C.T., and Sokol, D., "Laser Bond Testing," *Materials Evaluation*, Vol. 67, No. 7, 2009, pp. 818–827.

22. Ecault, R., Boustie, M., Berthe, L., et al., "Development of a Laser Shock Wave Adhesion Test for the Detection of Weak Composite Bonds," *5th International Symposium on NDT in Aerospace*, Singapore, November 13–15, 2013.

23. Yang, S., Gu, L., and Gibson, R.F., "Nondestructive Detection of Weak Joints in Adhesively Bonded Composite Structures," *Composite Structures,* Vol. 51, 2001, pp. 63–71.

24. Perton, M., Blouin, A., and Monchalin, J.P., "Adhesive Bond Testing of Carbon-Epoxy Composites by Laser Shockwave," *Journal of Physics D: Applied Physics* Vol. 44, No. 3, 2011, p. 12.

25. Hirsekorn, S., "Nonlinear Transfer of Ultrasound by Adhesive Joints—a Theoretical Description," *Ultrasonics*, Vol. 39, No. 1, 2001, pp. 57–68.

26. Davies, P., Sohier, L., Cognard, J.Y., et al., "Influence of Adhesive Bond Line Thickness on Joint Strength," *International Journal of Adhesion and Adhesives* (UK), Vol. 29, No. 7, 2009, pp. 724, 736.

27. Hagemaier, D.J., "Adhesive-Bonded Joint," *Nondestructive Evaluation and Quality Control, ASM Handbook*, Vol. 17, 1992, pp. 610–640.

28. Ehrhart, B., Valeske, B., Muller, C.E., and Bockenheimer, C., "Methods for the Quality Assessment of Adhesive Bonded CFRP Structures—A Resume," 2nd International Symposium on NDT in Aerospace 2010, We.5.B2, 2010, p. 9.

29. Adams, R.D., "The Nondestructive Evaluation of Bonded Structures," *Construction and Building Materials*, Vol. 4, No. 1, 1990, pp. 3–8.

30. Adams, R.D. and Cawley, P., "A Review of Defect Types and Nondestructive Testing Techniques for Composites and Bonded Joints," NDT International, Vol. 21, No. 4, 1988, pp. 208–222.

31. Rose, J.L. "Ultrasonic Nondestructive Evaluation Technology for Adhesive Bond and Composite Material Inspection," *Adhesive Bonding*, Chapter 15, Plenum Press, New York, NY, 1991, pp. 425–448.

32. Light, G.M., Kwun, H., "Nondestructive Evaluation of Adhesive Bond Quality, State of the Art Review," NTIAC-89-1, 1989.

33. Topical Proceedings, "NDE of Adhesive Bonds and Bondlines," Papers presented at ASNT Fall Conference, Valley Forge, PA, 1989, p. 155.

34. Bardis, J., Kedward, K., "Effects of Surface Preparation on the Long-Term Durability of Adhesively Bonded Composite Joints," DOT/FAA/AR-03/53 Final Report, 2004, p. 91.

35. Russell, J.D., "Composites Affordability Initiative," *AFRL Technology Horizons*, Vol. 7, No. 3, 2006, p. 44.

36. Russell, J.D., "Composites Affordability Initiative: Transitioning Advanced Aerospace Technologies Through Cost and Risk Reduction," *The AMMTIAC Quarterly*, Vol. 1, Nov. 3, 2007, pp. 3–6.

37. Bossi, R. “NDE Challenges for Composite Aircraft,” A4A Conference Keynote Address, NDT Forum, Seattle, WA, 2012.

38. Frank, L., and Schmitz, G., “Ultrasonic Emission Method Enables Testing of Adhesive Bonds,” NASA Technical Reports Server, Document ID: 19660000340, 1966.

39. Rokhin, S.I., Hefets, M., and Rosen, M., “An Ultrasonic Interface-Wave Method for Predicting the Strength of Adhesive Bonds,” *Journal of Applied Physics*, Vol. 52, 1981, pp. 2847–2851.

40. Hodges, W.T., Tyeryar, J.R., and Berry, M., “Bonding and Nondestructive Evaluation of Graphite/PEEK Composite and Titanium Adherends With Thermoplastic Adhesives,” Society of Manufacturing Engineers, Conference on Fabricating Composites, Hartford, CT, 1985.

41. dos Reis, H.L.M., and Krautz, H.E., “Nondestructive Evaluation of Adhesive Bond Strength Using the Stress Wave Factor Technique,” Glenn Research Center, NASA Technical Reports Server, Document ID: 19870044926, 1986.

42. Smith, A.C., and Yang, H., “Ultrasonic Study of Adhesive Bond Quality at a Steel-to-Rubber Interface by Using Quadrature Phase Detection Techniques,” Langley Research Center, NASA Technical Reports Server, Document ID: 19900030964, 1989; also Materials Evaluation Vol. 47, 1989, pp. 1396–1400.

43. Mal, A.K., Lih, S.S., and Bar-Cohen, Y., “Nondestructive Characterization of Adhesive Bonds from Guided Wave Data,” Proceedings of the 17th Annual Adhesion Society Meeting, Orlando, FL, 1994, pp. 262–265.

44. Chance, R., “Nondestructive Inspection (NDI) of Reduced Strength Bonds,” DOT/FAA/CT-93/42, 1994.

45. Lih, S.S., Mal, A.K., and Bar-Cohen, Y., “Ultrasonic Evaluation of Thermal Degradation in Adhesive Bonds,” Review of Progress in QNDE, Snowmass Village, CO, 1994, pp. 1–8.

46. Bar-Cohen, Y., Mal, A.K., and Lih, S.S., “NDE of Composite Materials Using Ultrasonic Oblique Insonification,” *Materials Evaluation*, Vol. 51, No. 11, 1993, pp. 1285–1296.

47. Rose, J.L., Rajana, K.M., and Hansch, M.K.T., “Ultrasonic Guided Waves for NDE of Adhesively Bonded Structures,” *Journal of Adhesion*, Vol. 50, 1995, pp. 71–82.

48. Brotherhood, C.J., Drinkwater, B.W., and Guild, F.J., “The Effect of Compressive Loading on the Ultrasonic Detectability of Kissing Bonds in Adhesive Joints,” Review of Quantitative Nondestructive Evaluation, edited by D.O. Thompson and D.E. Chimenti, Vol. 20, 2001, pp. 1111–1118.

49. Brotherhood, C.J., Drinkwater, B.W., and Guild, F.J., "A Comparison of the Detectability of Dry Contact Kissing Bonds in Adhesive Joints Using Longitudinal, Shear and High Power Ultrasonic Techniques," *Review of Quantitative Nondestructive Evaluation*, Thompson, D.O. and Chimenti, D.E., eds., Vol. 22, 2003, pp. 1033–1040.

50. Qu, J., "Ultrasonic Nondestructive Characterization of Adhesive Bonds," Langley Research Center, NASA Technical Reports Server, Document ID: 19990046400, 1999.

51. Nagy, P.B., McGowan, P., and Adler, L., "Acoustic Nonlinearities in Adhesive Joints," Review of Progress in QNDE, Vol. 9, 1991, pp. 1685–1692.

52. Achenbach, J.D., and Parikh, O.K., "Ultrasonic Analysis of Nonlinear Response and Strength of Adhesive Bonds," *Journal of Adhesion Science and Technology*, Vol. 5, No. 8, 1991, pp. 601–618.

53. Parikh, O.K. and Achenbach, J.D., "Analysis of Nonlinearly Viscoelastic Behavior of Adhesive Bonds," *Journal of Nondestructive Evaluation*, Vol. 11, 1992, pp. 221–226.

54. Hirose, S. and Kitahara, M., "Time Domain BIE Applied to Flaw Type Recognition," Review of Progress in QNDE, Vol. 10A, 1992, pp.75–82.

55. Anastasi, F. and Roberts, M.J., "Acoustic Wave Propagation in an Adhesive Bond Model With Degrading Interfacial Layers," MTL TR 92-63, U.S. ARMY Materials Technology Laboratory, 1992.

56. Pangraz, S. and Arnold, W., "Quantitative Determination of Nonlinear Binding Forces by Ultrasonic Technique," Review of Progress in QNDE, Vol. 13B, 1994, pp. 1995–2001.

57. Tang, Z., Cheng, A., and Achenbach, J.D., "An Ultrasonic Technique to Detect Nonlinear Behavior Related to Degradation of Adhesive Bonds," Review of Progress in QNDE, Vol. 16, 1997.

58. Berndt, T.P., Green, Jr., R.E., "Investigation of Adhesive Bond Cure Conditions Using Nonlinear Ultrasonic Methods," *Proceedings of the Second Annual Symposium for Nondestructive Evaluation of Bond Strength*, sponsored by NASA at Langley Research Center, Hampton, VA, 1999.

59. Berndt, T.P. and Green, R.E., "Feasibility Study of a Nonlinear Ultrasonic Technique to Evaluate Adhesive Bonds," Private Communication, 1998.

60. Lowe, M.J.S. and Cawley, P., "The Applicability of Plate Wave Techniques for the Inspection of Adhesive and Diffusion Bonded Joints," *Journal of Nondestructive Evaluation*, Vol. 13, 1994, pp. 185–199.

61. Rose, J.L., Zhu, W. and Zaidi, M., "Ultrasonic NDT of Titanium Diffusion Bonding With Guided Waves," *Materials Evaluation*, Vol. 56, No. 4, 1998, pp. 535–539.

62. Cantrell, J.H., "Fundamentals and Applications of Nonlinear Ultrasonic Nondestructive Evaluation," in Kundo, T., *Ultrasonic Nondestructive Evaluation: Engineering and Biological Material Characterization*, CRC Press, London, ISBN: 9780203501962, 2003, pp. 363–433.

63. Zheng, Y., Maev, R.G., and Solodov, I.Y., "Nonlinear Acoustic Applications for Material Characterization: A Review," *Canadian Journal of Physics*, Vol. 77, 1999, pp. 927–967.

64. Heyman, J.S. and Lynch, J.E., "Bond Testing System, Method and Apparatus," U.S. Patent Publication Number: US7017422 B2, 2006.

65. Yan, D., Drinkwater, B.W., and Neild, S.A., "Measurement of the Ultrasonic Nonlinearity of Kissing Bonds in Adhesive Joints," NDT&E International, Vol. 42, 2009, pp. 459–466.

66. Yan, D., Drinkwater, B.W., and Neild, S.A., "Experimental and Theoretical Characterization of Kissing Bonds in Adhesive Joint Using Non-Linear Ultrasonic Measurement," *Review of Quantitative Nondestructive Evaluation*, Thompson, D.O. and Chimenti, D.E., eds., Vol. 29, 2010, p. 1190–1197.

67. Yan, D., Drinkwater, B.W., and Neild, S.A., "Modelling and Measurement of the Nonlinear Behaviour of Kissing Bonds in Adhesive Joints," NDT&E International, Vol. 47, 2012, pp. 18–25.

68. Jian, X., Guo, N., Dixon, S., and Grattan, K.T.V., "Ultrasonic Weak Bond Evaluation in IC Packaging," *Measurement Science Technology*, Vol. 17, 2006, pp. 2637–2642.

69. Stratoudaki, T., Hernandez, J.A., Clark, M., and Somekh, M.G., "Cheap Optical Transducers (CHOTs) for Narrowband Ultrasonic Applications," *Measurement Science and Technology*, Vol. 18, 2007, pp. 843–851.

70. Klein, M., "Laser Ultrasonic Inspection of Adhesive Bonds Used in Automotive Body Assembly," DOE Final Report on USCAR NDI, 2010, pp. 10–11 to 10–17.

71. Nagy, P.B. and Adler, L., "Nondestructive Evaluation of Adhesive Joints by Guided Waves," *Journal of Applied Physics*, Vol. 66, No. 10, 1989, pp. 4658–4663.

72. Nagy, P.B., "Nonlinear Imaging for Enhanced Ultrasonic Assessment of Diffusion Bonded Engine Components," Proposal Submitted to FAA, Solicitation Number: 11825, 2012, p. 11.

73. Jones, G.L. and Kobett, D.R., "Interaction of Elastic Waves in an Isotropic Solid," *Journal of the Acoustic Society of America*, Vol. 35, 1963, pp. 5–10.

74. Rollins, F.R., "Interaction of Ultrasonic Waves in Solid Media," *Applied Physics Letters*, Vol. 2, 1963, p. 147.

75. Vijaya Kumar, R.L., Bhat, M.R., and Murthy, C.R.L., "Some Studies on Evaluation of Degradation in Composite Adhesive Joints Using Ultrasonic Techniques," *Ultrasonics*, 2013, http://dx.doi.org/10.1016/j.ultras.2013.01.014 (accessed on 10/06/2014).

76. Zaitsev, M.B., "Influence of 'Weak' Bonds in Macromolecules on the Activation Energies of Fracture of Oriented Polymers," *Polymer Science USSR*, Vol. 28, No. 2, 1986, pp. 392–397.

77. Rantala, J., Wu, D., and Busse, G., "Amplitude-Modulated Lock-in Vibrothermography for NDI of Polymers and Composites," *Research in Nondestructive Evaluation*, Vol. 7, 1996, pp. 215–228.

78. Meola, C., Carlomagno, G. M., and Giorleo, G., "Using Infrared Thermography to Analyze Substrate and Adhesive Effects in Bonded Structures," *Journal of Adhesion Science and Technology*, Vol. 18, No. 6, 2004, pp. 617–634.

79. Genest, M., Martinez, M., Mrad, N., Renaud, G., and Fahr, A., "Pulsed Thermography for Non-Destructive Evaluation and Damage Growth Monitoring of Bonded Repairs," *Composite Structures* (UK), Vol. 88, No. 1, 2009, pp. 112–120.

80. Renshaw, J., Holland, S.D., Thompson, R.B., and Uhl, C., "The Effect of Crack Closure on Heat Generation in Vibrothermography," *Review of Progress in Quantitative Nondestructive Evaluation*, Thompson, D.O. and Chimenti, D.E., eds., Vol. 28, 2009, pp. 473–480.

81. Holland, S.D. and Vaddi, J., "Viscoelastic Absorptive Coatings for Vibration Coverage Analysis in Vibrothermography," *Review of Progress in Quantitative Nondestructive Evaluation*, Thompson, D.O. and Chimenti, D.E., eds., Vol. 32, 2012, p. 11.

82. Sathish, S., Welter, J.T., Jata, K.V., Schehl, N., and Boehnlein, T., "Development of Nondestructive Non-Contact Acousto-Thermal Evaluation Technique for Damage Detection in Materials," *Review of Scientific Instruments*, Vol. 83, No. 9, 2012, pp. 95–103.

83. Myers, R.S., "NDE of Thermal Protection System for Space Shuttle Solid Rocket Booster," Johns Hopkins University, *The 1990 JANNAF Propulsion Meeting*, Vol. 2, 1990, pp. 1–10.

84. Shankar, K., Fei, D., "Modelling of Weak Bonds in Adhesively Fastened Joints," The Second Joint NASA/FAA/DoD Conference on Aging Aircraft, Williamsburg, VA, 1999.

85. Heslehurst, R.B., "Optical NDT of Adhesively Bonded Joints," *Materials Evaluation*, Vol. 67, No. 7, 2009, pp. 837–842.

86. Hewitt, R.R., "Nondestructive Testing of Adhesive Bonds by Nuclear Quadrupole Resonance Method," Marshall Space Flight Center, NASA Technical Reports Server, Document ID: 19710000207, 1971.

87. Greene, R.J., Patterson, E.A., and Rowlands, R.E., "Thermoelastic Stress Analysis," *Springer Handbook of Experimental Solid Mechanics*, Sharpe, W.Nl, ed., 2008, pp. 743–768.

88. Abou-Khousa, M.A., Ryley, A., Kharkovsky, S., et al., "Comparison of X-Ray, Millimeter Wave, Shearography and Through-Transmission Ultrasonic Methods for Inspection of Honeycomb Composites," *Review of Quantitative Nondestructive Evaluation*, Thompson, D.O. and Chimenti, D.E., eds., Vol. 26, 2007, pp. 999–1006.

89. Pethrick, R.A., Hayward, D., McConnell, B.K., and Crane, R.L., "Use of High and Low Frequency Dielectric Measurements in the NDE of Adhesively Bonded Composite Joints," *Proceedings of the SPIE - The International Society for Optical Engineering*, Vol. 5767, No. 1, 2005, pp. 55–65.

90. Davis, G.D., Mani, S., Rich, M.J., and Drzal, L.T., "Electrochemical Impedance Spectroscopy Inspection of Composite Adhesive Joints," *Journal of Adhesion Science Technology*, Vol. 19, No. 6, 2005, pp. 467–492.

91. Anderson, G.P., Bennett, S.J., and DeVries, K.L., "Analysis and Testing of Adhesive Bonds," Academic Press, New York, NY, 1977.

92. Pocius, A.V., "Adhesion and Adhesives Technology, An Introduction," 2nd Edition, Hanser Publications, Cincinnati, OH, 2011.

APPENDIX A—METAL-TO-METAL ADHESIVE BONDING PROCESS DOCUMENT

Table A-1. Metal-to-Metal Adhesive Bonding Process Document

WORK PROCEDURE

Metal Adhesive Bonded Repair Test Specimen Preparation

Organization	Name, Dept	Signature	Date
Document Custodian	Carl L. Jacques		
Document Owner: SNL/NM	Carl L. Jacques		
Author/Process Owner: SNL/NM	Michel Bode		
Approved by: 6621 Quality Assurance Reviewer	Stephen Neidigk		

CONTROL NUMBER	ISSUE	DATE	EXPLANATION OF CHANGES
Work Procedure - Aluminum Bonded Repair	Draft	11/09/2012	Preliminary

A-1. INTRODUCTION

This work procedure in table A-1 outlines the multi-tiered process of generating aluminum-to-aluminum metal alloy adhesive bonded specimens simulating repairs to transport airplanes. The results will be samples with repeatable and controlled mechanical strengths used in destructive and nondestructive testing to measure bond strength.

Specimens are prepared in accordance with aerospace industry adhesive bonded repair specifications from airplane and adhesive manufacturers, as well as the ASTM D 3165-07 Single Lap Shear Test Standard and ASTM D 3762-98 Wedge Test Standard. Specimens are fabricated in designated batch lots. Each lot contains recordable material accountability and process fabrication parameter accountability (e.g. cure temperatures, cure times, processing equipment calibrations, and batch mix information for consumables), as well as process variable values for fabrication parameters (presence of contaminants, changes in cure temperatures and times, etc.).

A-1.2 PURPOSE

The purpose of this work is to describe and define the procedures used for material selection, surface preparation, bonding methodology, curing, and destructive and nondestructive test parameters. These procedures and associated quality records are intended to be implemented for all levels and variations of specimen fabrication and testing.

A-2. KEY DEFINITIONS

AANC – Airworthiness Assurance NDI Validation Center
ARP – Aerospace Recommended Practice
SNL NM – Sandia National Laboratories, New Mexico
SRM – Structural Repair Manual
TATS – Time and Temperature Sensitive
TDS – Technical Data Sheet
CCA – Controlled Contamination Area

A-3. PREREQUISITES

A-3. REFERENCES

Table A-2.

Always use latest released documents.

Document No.	**Description**
Boeing 767-400 SRM 51-70-1, p. 239	Structural Repair Manual
AIR 2012-10-31 (Proposed Draft)	Guidelines for Repair Process
ASTM D 3762-98	Standard Test Method for Adhesive-Bonded Surface Durability of Aluminum (Wedge Test)
ASTM D 3165-07	Standard Test Method for Strength Properties of Adhesives in Shear by Tension Loading of Single-Lap-Joint Laminated Assemblies
3M Surface Pre-Treatment AC-130 (Boegel)	Technical Data Sheet and Application Guide
Cytec BR 6747-1 Bonding Primer	Technical Data Sheet and Application Guide
SNL NM Procedure ESH100.2.ENV.22	Control Document for Waste Management
Boeing Bonded Repair Document	Materials & Processes
ASTM D 3933-98 (Reapproved 2010)	Standard Guide for Preparation of Aluminum Surfaces for Structural Adhesives Bonding (Phosphoric Acid Anodizing)

A-3.2 EQUIPMENT AND MATERIALS

Personal Protective Equipment		
Qty.	Equipment ID	Description
1 pair	NONE	Nitrile or Latex Gloves (all sizes)
1	NONE	Approved Safety Glasses OR
1	NONE	Chemical-Resistant Splash Face Shield
1 Pair	NONE	Approved Hearing Protection

Required Equipment		
Qty.	Equipment ID	Description
1	Fume Hood	Certified Air Flow
1	Bake out Oven	Calibrated, Programmable
1	Digital Thermometer	Calibrated, Recordable, Data Download (Data Logger)
1	Vacuum System	Venturi Vacuum System Fitting, High Temperature Hoses, Calibrated Monitoring Gauge, Capable of -14 in Hg
4	Monitoring	"T" or "K" Type Thermocouples
1	Monitoring	Thermometer/Humidity indicator
1	Random Orbital Sander	Material Sanding Preparation
2	Caul Plates	Aluminum Plate 24″ x 24″ x 0.25″
1	Table Saw & Blade	Carbide Triple Facet 120 Tooth 0.064" Cut Path
1	Band Saw & Blade	Metal cutting blade
1	IR Heat Thermometer	IR Temperature Indicator, Digital Readout
1	Timer	Minute Timer for Specified Durations
1	Vacuum	Removal of Sanding Dust
1	Coating Thickness Measurement Tool	PosiTector Eddy Current Coating Measurement Tool

Materials Quantity	Material Identification	Description
As Needed	Airtech Release Film	Roll, release film, Blue, 0.001, ″ PN WL5200B-001
As Needed	Airtech Release Film	Roll, release film, Red, 0.002″ Perforated, PN A4000R260208P
As Needed	Airtech Vacuum Tape	Tape, 1.00″ Blue, 0.002″ Vacuum, Airtech Part # FB1172
As Needed	Airtech Vacuum Seal	Seal Tape, Yellow, 1/2″ Wide, PN AT200Y, 1/2″ x 25 Feet
As Needed	Airtech Peel Ply or Fiberglass Cloth	120-Fiberglass Cloth or Nylon Peel Ply as Intermediate Bleeder Layer
As Needed	Airtech Ultra Weave	Vacuum Bleeder Material, 60″ Wide, PN UW6066050
As Needed	Cerex Fabric	Positioning Cloth Between Adhesive Film and Plates, PN
As Needed	Airtech Bagging Film	Roll, Bagging Material, Green, 0.008″, PN Wl7400-002
1 (per plate)	Sanding Discs	180 Grit, Aluminum Oxide, 5″ Round, Merit
As Needed	125 mL Squirt Bottles	Dispensing Primer/Chemicals

Materials Quantity (continued)	Material Identification	Description
As Needed	3M AC 130 (Boegel)	Surface Pre-Treatment 50 ml 4 part kits
As Needed	3M AF163-2k.06M	Pre-Preg Adhesive Film, 0.0095," Red, Reinforced
As Needed	Approved	Lint Free Wipes
As Needed	Brush	Black Foam, Disposable

IR=infrared

A-3.3 RECORDS/DOCUMENTATION

By performing this procedure, the operator acknowledges that he/she has read, understands, and recognizes the requirements, processes, and safety concerns stated in this procedure. Only individuals who have read and signed the Authorized Users List (appendix A) and have process owner certification may perform the procedures listed in this work instruction.

Results of this work instruction shall be recorded on the attached and supplemental Batch Traveler Log. Any visual defects, discrepancies, or issues shall be annotated in the notes of the fabricator and detailed in attachments for each specific sub-process.

A-3.4 TRAINING

There is specific on-the-job training for performing this process in the form of individual job safety analyses. Additionally, to ensure fabrication quality standards are met, process owners must certify that operators are qualified to perform this process in accordance with this work procedure. The process owner will ensure that all associated technical and safety training is complete and have the operator demonstrate competence on the equipment and processes of each fabrication step and subject JSA. Qualified operators are authorized to conduct work by signature of themselves and the process owner on the Authorized Operator List in the appendix.

A-3.5 WASTE MANAGEMENT

Waste management is controlled in accordance with Sandia National Laboratories, New Mexico (SNL, NM) procedures and processes for generation, reduction, elimination, and removal of hazardous waste. Reference SNL NM Procedure ESH100.2.ENV.22.

A-3.6 LABORATORY ENVIRONMENT — CONTROLLED CONTAMINATION AREA

All attempts are made to reduce particulate count and maintain a clean and dust-free work condition. Workers will wear long pants, closed-toe shoes, and outer lab coats at all times, and through best work practices will attempt to limit unwanted contamination by unwanted sources, such as body fluids, hair, etc. The temperature within the laboratory should remain at 75° F (+/- 5°) at all times. Humidity levels and temperature will be monitored and recorded prior to, during, and at completion of processing. Only tools, materials, and equipment designated for use

in the controlled contamination area **(**CCA) are allowed. Eating and drinking in the CCA are never allowed.

A-3.7 LABORATORY CLEANING PROCEDURE

This procedure must be completed prior to the introduction of any sample components and before production of test samples. The purpose is to control and eliminate unwanted sources of contamination.

1. Nitrile gloves must be worn at all times: Avoid cross contamination of tools and equipment.

2. The floor must be wet-mopped and allowed to dry at least 2 hours prior to fabrication. DO NOT SWEEP OR VACUUM in the lab.

3. Wipe all surfaces with pre-moistened isopropyl alcohol (IPA) wipes. Wipe in one direction to remove dust and debris from primary work area. DO NOT USE COMPRESSED AIR to clean inside the work area.

4. Wipe the work surfaces, the fume hood, the cutting table top, the top of the freezer, all tools, and all containers.

5. Keep all doors closed during cleaning and fabrication operation.

6. Prohibit any penetrant or magnetic particle inspection (adjacent room) during the cleaning and fabrication processes.

7. Prohibit any shop metal fabrication work (adjacent room) that involves cutting, grinding, or welding during the cleaning and fabrication processes.

A-3.8 RESTRICTED ACCESS TO LABORATORY

Only authorized workers who have read and signed this work procedure are allowed to perform fabrication processes. Entry and exit to and from the lab shall occur only through the swinging double doors on the southwest wall. Opening the north door into the shop area is prohibited during fabrication. If emergency egress is necessary, leave the lab by the nearest exit door, ensuring that the doors close upon exit.

A-4. PROCEDURE

A-4.1 MATERIAL SELECTION AND PROCESSING

Assembled plates will be constructed from sheet material sheared to dimensions defined in ASTM D 3762 and ASTM D 3165-07 for both wedge test specimens and single lap shear test specimens, respectively. Materials are identified in ASTM D 3762 and ASTM D 3165-07 as 2024 T3 bare sheet, 0.063″ thickness (lap shear), and 0.125″ thickness (wedge test specimens). Use 2024-T3 bare-sheet aluminum for the base portion of panels that simulate existing airplane

structure being repaired and 2024-T3 bare that has undergone phosphoric acid anodization (PAA) and spray primer for the top portion of panels that simulate repair patches.

A-4.1.1 Shear material to dimensions as follows (per batch):

1. Sheet material should be clean and free of grease, oil, debris, or other gross contaminants that would interfere with shearing and sanding.

2. Quantity: 1 each bare and PAA, 9.00″ ± 0.20″ x 9.00″ ± 0.20″ (0.063″ material thickness) for one batch lot of single lap shear specimens.

3. Quantity: 2 each bare and PAA, 6.00″ ± 0.125″ x 7.00″ ± 0.125″ (0.125″ material thickness) for one batch lot of wedge test specimens.

4. All edges of the metal panels and specimens must be flat, free of burrs, and reasonably smooth.

A-4.2 CLEANING OF PLATES PRIOR TO SANDING OPERATION

1. Acetone cleaning prior to sanding plates must be performed inside the CCA; USE FUME HOOD FOR CLEANING with acetone. The purpose of this cleaning step is to remove dirt, oil, grease, and other gross contamination prior to sanding.

2. Wearing nitrile gloves and using lint-free wipes and a clean, designated acetone source*, complete the following steps for each plate:

    a) Fold the wipe as shown to achieve a clean area of material for each stroke.

    b) Wet the wipe with clean acetone. Use the applicator bottle. NEVER put the cloth to the acetone source.

    c) Using the wipe, apply even pressure and a single, one-direction-only motion. DO NOT use circular or random wiping motions.

    d) For each stroke, refold the cloth as shown and repeat the wipe motion until there is no residue seen on each new surface of the cloth.

    e) Do not reuse the solvent or wipes. Use a clean wipe and fresh solvent for each plate.

    f) Allow to air dry for at least 5 minutes in the fume hood with the exhaust turned on.

    *Use acetone containers labeled “final clean only.” Do not pour acetone from the can onto a wipe. Use an approved chemical applicator bottle. NEVER return used acetone to a “final clean only” container.

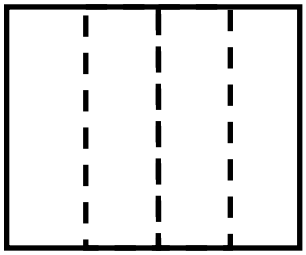

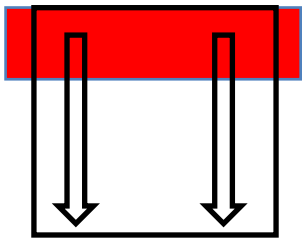

Fold the wipe as shown for clean surfaces. Pull the wipe in one direction only.

3. Always use clean nitrile or latex gloves when handling plates after cleaning.

4. If moisture is present, use the oven to dry prior to further processing.

5. Do not perform a water break test.

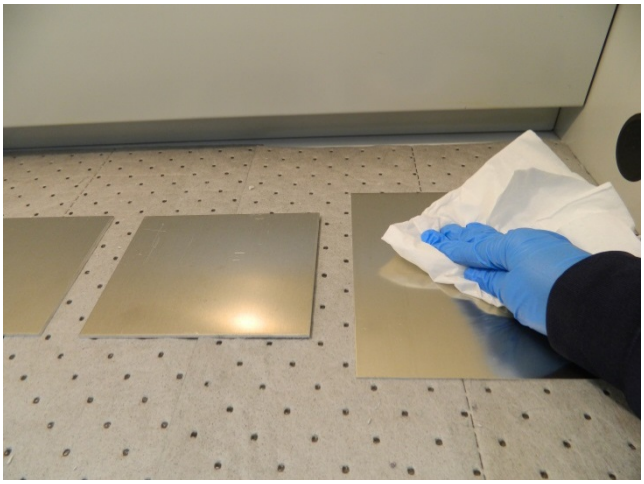

A-4.3 SURFACE SANDING

This is a critical procedure, which is necessary for removal of the metal oxide layer on the aluminum and to make the surface reactive for the AC-130 surface application.

Sanding must be accomplished OUTSIDE of the clean room area used for bond preparation. Immediately after sanding, clean all plates with pressurized air (with no greater than 30 psi) prior to entering the clean preparation area. Make sure to clean all edges and remove as much residue as possible.

A-4.3.1 The repair surface shall be prepared for AC-130 application by sanding it in accordance with Boeing 767-400 SRM 51-70-1, p. 239; alternate MD80 SRM 51-70-2, p. 260; or other Boeing-approved application instructions.

A-4.3.2 The surface preparation/sanding area shall extend to the edges of all plates.

A-4.3.3 The sanding mechanism specified is a random orbital sander utilizing aluminum oxide base 180-grit sandpaper.

Sandpaper MUST be 180-grit and one of the approved products (Merit Shur Stik ALO Resin Bond or 3M Stikit Sanding Disks). Different grit numbers can cause damage to the metal surface or will not remove all the oxidation. Different grit, paper, or adhesive materials can cause an unsatisfactory chemical bond between the AC-130 and bare metal surfaces (see "Boeing Bonded Repair—Materials & Processes" document for further details).

After completion of the sanding and cleaning process, pre-treatment AC-130 solution must be applied as soon as possible (AC-130 Application Guide recommends within 30 minutes), within no later than 8 hours (Boeing SRM 767-400 51-70-1 p. 239).

Note the sanding start time in the batch lot traveler.

A-4.3.4 For each 9″ x 9″ or 6″ x 7″ plate, the following method and protocol must be followed:

1. Make sure the sander will not get oil contamination on the sandpaper or bond surface.

2. Use a vacuum to extract dust particles during operation or perform work on a downdraft table if the sander does not have a vented or filtered exhaust.

3. Use a new sheet of sandpaper for each plate. Do not reuse sanding discs.

4. Provide 1 minute of continuous sanding to each plate.

5. Use a digital scale to achieve approximately 20 lb. of sanding pressure in conjunction with the use of a digital timer to accurately keep count of elapsed time.

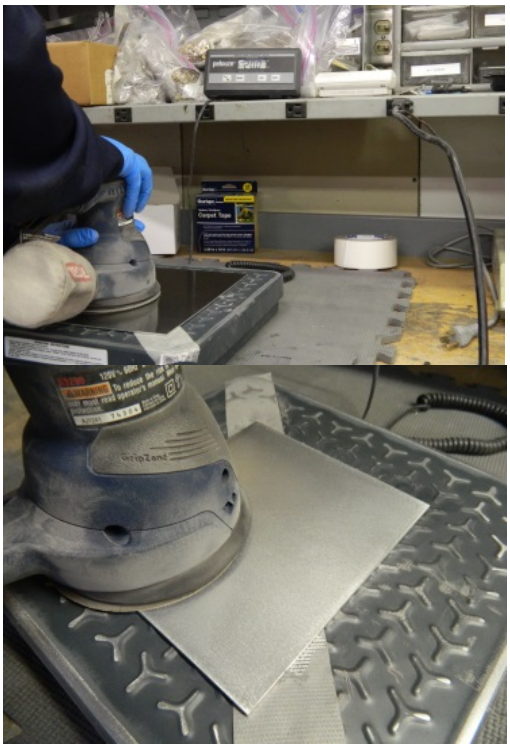

6. Apply double-sided adhesive carpet tape to the digital scale to ensure the plate does not slide during the sanding process. Note: 9″ x 9″ panels must be sanded first. The aluminum particles will cover the carpet tape and make it unusable if the 6″ x 7″ panels are sanded first.

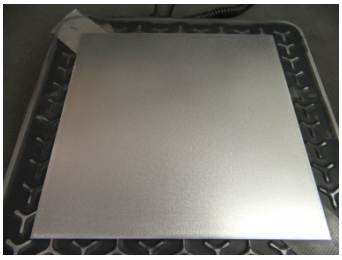

7. Using a new sheet of specified sand paper, guide the sander side-to-side using 20 lb. of total pressure, covering the surface uniformly, and overlapping the previous sanding path. Once sanding is completed in one direction, change direction by 90 degrees to achieve one cross coat. Continue for 1 minute while vacuuming dust particles.

8. Sanding must extend over the plate edges for uniform coverage.

9. Change the sand paper if it gets torn or clogged.

10. Clean debris from the plate using filtered pressurized air, with a pressure not to exceed 30 psi.

A-4.4 HANDLING OF PROCESSED PLATES

1. DO NOT STACK PLATES.

2. Minimize the amount of handling of the plate, especially in the middle. The plates should be handled by the edges only in the drop-off cutting zones.

3. Move all plates into the fume hood in the CCA as soon as sanding and pre-cleaning are done.

4. Protect each sanded surface from airborne and contact contaminants.

5. If the plate becomes contaminated, solvent cleaning (with acetone) is required, followed by another sanding.

6. DO NOT REUSE SOLVENT, WIPES, OR SANDPAPER DISKS.

A-4.5 MIXING AND APPLICATION OF AC-130 PRE-TREATMENT (BOE-GEL) SOLUTION

1. Mix all components EXACTLY as noted within each kit instruction: All components must be thoroughly agitated prior to mixing.

2. AC-130 pre-treatment has a limited pot life of only 10 hours from mixture time.

3. A new brush or roller and dispensing pipette MUST be used for each batch.

4. Mix according to instructions and allow 30 minutes of “induction” time to elapse before application.

5. Recommended temperature for mix and cure is 57° F to 87° F and humidity must be <85% RH.

6. Using the Batch Lot Traveler, record the AC-130 batch number, expiration date, time mixed, temperature, humidity, and the time the application was completed.

A-4.6 MIXING INSTRUCTIONS: AC 130 SURFACE PRE-TREATMENT 50 ML FOUR-PART KIT

If more than 50 ml is required, only containers having the same lot numbers should be mixed. Mix each kit separately and then combine before application to plates.

1. Dispense part A into part B and shake for 15 seconds. If there are white particles in the mixture, DO NOT USE.

2. Dispense part C into part D and shake for 15 seconds.

3. Pour part B mixture from step 1 into part D mixture from step 2 and shake for 15 seconds.

4. Allow the mixed material to sit for 30 minutes.

5. If solution remains cloudy, DO NOT USE.

6. Prior to use, shake mixture for 15 seconds.

A-4.7 APPLICATION INSTRUCTIONS: AC 130 SURFACE PRE-TREATMENT 50 ML FOUR PART KIT

1. Place panels on the Boe-Gel table. Lift up the panel and place on the edge of the cart, raising it to an approximately 30–35 degree angle.

2. Using a new disposable pipette, dispense AC-130 solution onto the panels and spread evenly over the surface with a new and clean foam brush or roller.

3. Maintain continuous 100% surface wetting for 2 full minutes.

4. After 2 minutes, place the plates in the drying rack to allow excess solution to drain, being careful not to allow the cart or adjacent panels to touch the finished surfaces except around the edges. Do not blot, brush, rub, or wipe any excess solution.

5. Allow a minimum of 1 hour ambient drying time.

6. Primer (the next step) must be applied within 24 hours of the AC-130 pre-treatment application.

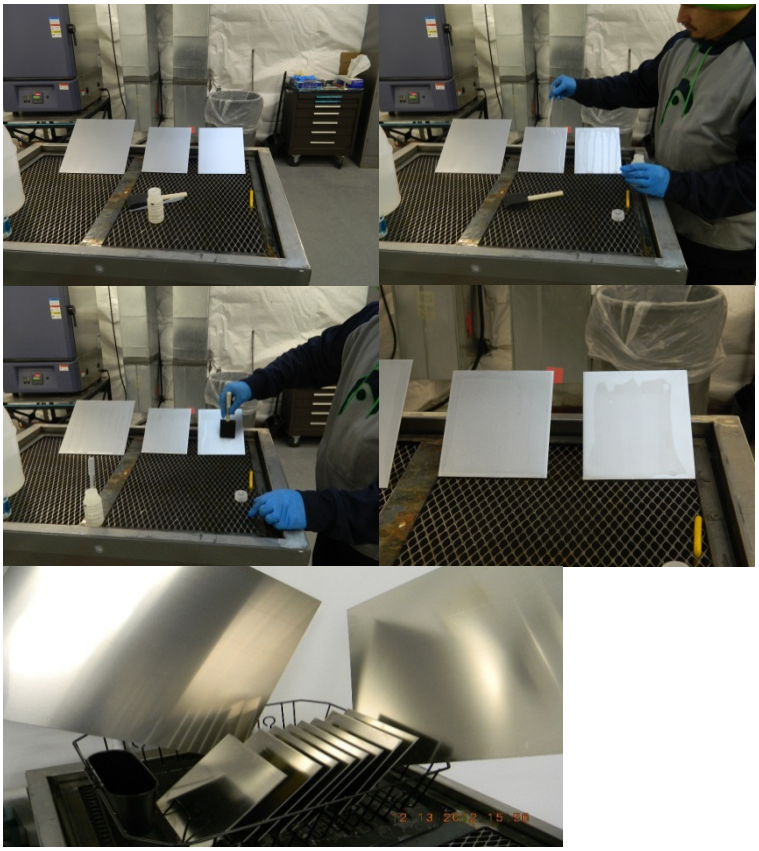

A-5. APPLICATION AND CURING OF CYTEC BR 6747-1 BONDING PRIMER ON NON-PAA ALUMINUM PLATES

Cytec BR 6747-1 primer contains hexavalent chromate ion, which is toxic and carcinogenic. Consult MSDS prior to use and wear appropriate PPE during application of liquid primer.

Cytec BR 6747-1 Primer is stored at 40°F to 55°F and must be warmed to an ambient temperature prior to use. To minimize contamination of the pint container, extract an aliquot of primer into a smaller bottle after stirring; remove only one aliquot for each batch. Thorough agitation is required to break up the heavy solids settled on the bottom prior to use. Use a new disposable pipette or dedicated stirring rod to break up the solids PRIOR to dispensing an aliquot for immediate use. After thorough mixing, the primer should maintain a cloudy appearance.

During primer application, the bottle must be constantly agitated by stirring while dispensing primer onto the prepared surface.

A-5.1 APPLICATION OF CYTEC BR6747-1 BONDING PRIMER

1. Use noncontact infrared (IR) temperature gage to determine that primer temperature is 65° to 95°F.

2. Wearing nitrile gloves, remove plates from the AC-130 drying area and return them to the primer application workstation. Plates should be laid flat on the elevated stand-off holders to avoid contamination from dragging the brush or roller onto the work area.

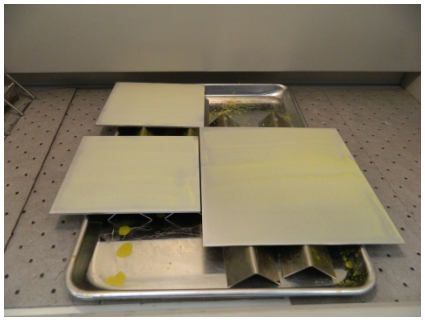

3. After verifying the primer is at ambient temperature, agitate the container continuously to ensure all deposits are mixed and will stay mixed during application.

4. Using a new, clean, disposable pipette, dispense the Cytec BR 6747-1 primer onto the plates.

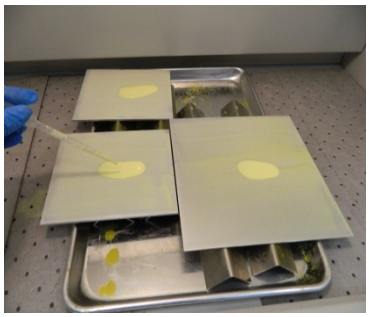

5. Using a new clean foam brush or roller, spread the primer with alternating horizontal and vertical strokes, ensuring continuous full coverage of plates for 1 full minute. Continue to agitate the primer container during dispensing.

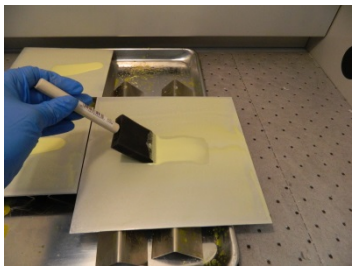

6. Allow the primer to air dry at ambient temperature (<55% relative humidity) for 15–60 minutes until no surface moisture is present.

7. To achieve correct material thickness, two primer coats must be applied. A drying period and short oven cure follows each primer coat (15 minutes at 160°F after initial air dry).

8. Using clean nitrile gloves, transfer the plates into the adjacent preheated oven for 15 minutes at 160°F.

9. Remove the plates from the oven and allow them to cool to ambient temperature. Once cooled, repeat primer application as noted above. Primer requires continuous agitation during application.

10. Color is an indication of primer thickness and should appear even over the entire plate surface. Noticeably thick or thin areas based on color are cause for plate rejection and replacement.

11. After the final coat of primer has air dried at ambient temperature, transfer the plates into the preheated curing oven and bake for 60 minutes at a plate temperature (not oven

temperature) of 250°F. Use the temperature data logger and thermocouples to monitor plate temperature.

A-5.2 OVEN-CURING CYTEC BR 6747-1 PRIMER

Plates treated with Cytec BR 6747-1 primer require a heat-cure process of 60 minutes at 250°F +/- 10°F (121°C +/- 5.6°C) in accordance with Cytec Technical Data Sheet AEAD-00017, Rev: 0, 04/13/2010).

1. Turn on the small curing oven in the CCA and preheat to 250°F +/- 10°F (121°C +/- 5.6°C).

2. Place the primed plates on the primer curing rack in the oven for 1 full hour.

3. After 1 hour has elapsed, turn off the oven and crack open the door, allowing approximately 45 minutes for the plates to cool.

4. Use the IR thermometer to verify the plate temperature is less than 100°F prior to removal.

5. Once the plates have cooled, measure primer thickness using the PosiTector Eddy Current coating thickness measurement instrument.

6. The PosiTector must be calibrated on a similar aluminum plate with the provided shims. See PoiTector operation manual for calibration instructions.

7. Once calibration is verified, obtain primer thickness at five points across the plate to ensure a uniform coating. Up to 50% variation from the target thickness of 0.0025″ is allowed.

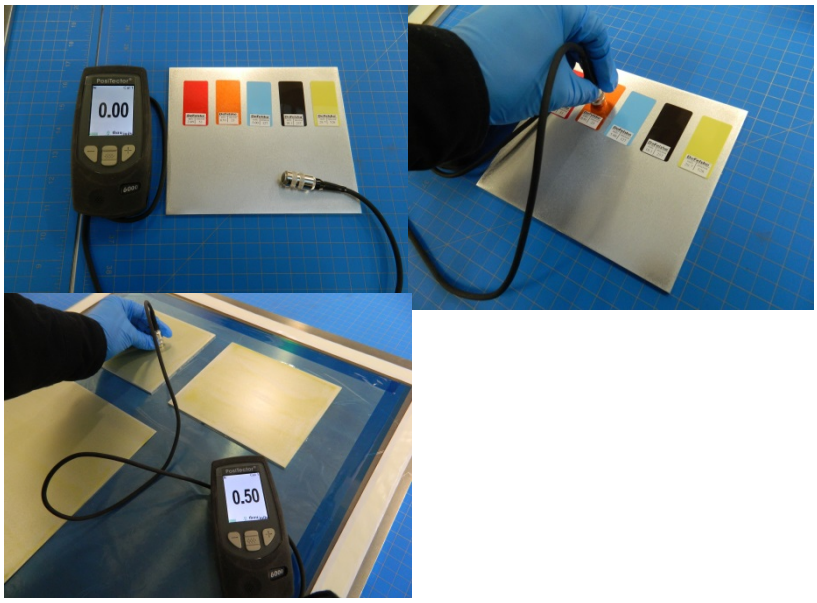

A-6. ADHESIVE FILM LAYUP PROCEDURE

All work must be completed within the CCA. All materials listed are specific to vacuum bagging and cure process; no substitutions are allowed without approval by the process owner. Perform a wipedown of all work surfaces and tools using IPA wipes before starting work.

Nitrile gloves must be worn while handling all tools and materials. All tools and work surfaces must be clean as well as oil- and dust-free. Every attempt must be made to keep materials from contacting any other surface that can cause contamination.

Each bonded specimen consists of two plates joined with adhesive film. One plate simulates the airplane side of a repair and undergoes processing similar to what might occur during an actual repair process in a maintenance hangar (see the bottom plate in figure A-5). This is the bottom plate shown below. It is prepared using the sanding, Boe-Gel, and primer application processes detailed in prior steps. The other plate simulates a repair patch plate that has been previously prepared by a commercial plating/coating shop vendor. It is the top plate in the diagram that has undergone a PAA process described in ASTM D3933-98, Standard Guide for Preparation of Aluminum Surfaces for Structural Adhesives Bonding (Phosphoric Acid Anodizing).

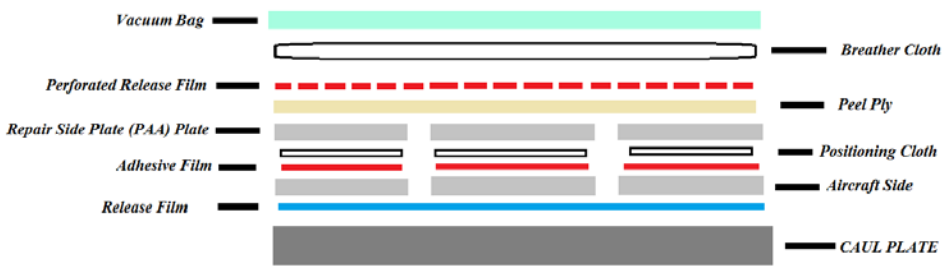

A-6.1 PREPARATION OF CAUL PLATE

1. Select a 24″ x 24″ x ¼″ caul plate and remove all previous bagging materials. Clean the caul plate with isopropyl alcohol wipes and inspect the plate for any surface scratches that may affect vacuum-sealing operations.

2. Cut a blue release film square approximately 2.0″ smaller than the perimeter of the plate and tape in place as shown. Leave ¾″ to 1.0″ bare surface for yellow sealing tape around the edges of the caul plate.

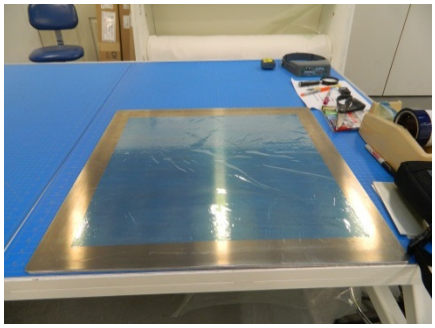

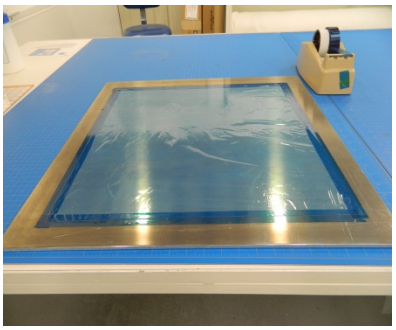

3. Seal the periphery of the caul plate at the bare metal surface using the 1/2″ yellow vacuum barrier tape. Use one continuous piece and overlap corner, as shown. Do not peel the paper backing from the upper portion of the barrier tape seal layer.

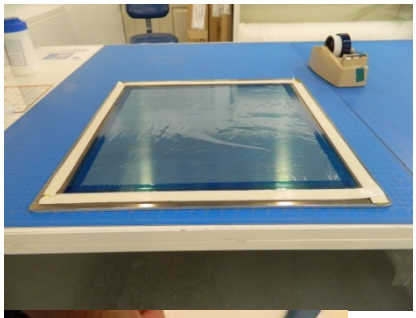

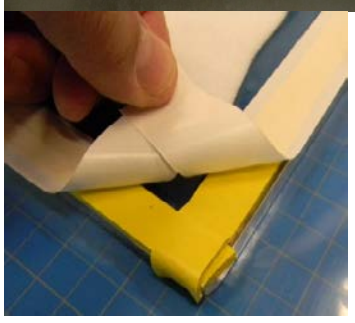

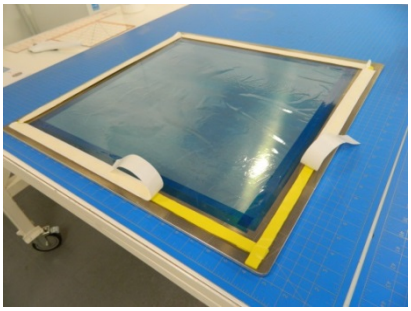

A-6.2 WEDGE TEST SPECIMEN LAYUP

1. Wearing nitrile gloves, arrange two primer panels (6″ x 7″ size) as shown by the two upper plates in the picture below. Apply three layers of blue flash breaker tape to the upper edge of each plate, covering the top ¾″ of the plate. These tape layers maintain bond line thickness of adhesive where there is no adhesive film; the wedge is driven for strength testing.


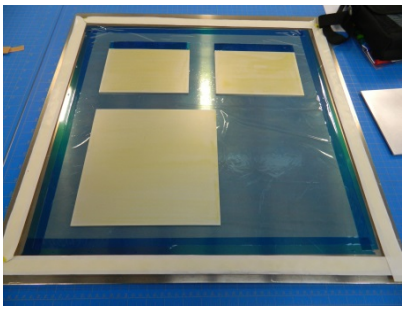

2. Adhesive film (3M AF-163-2, red) is kept frozen prior to use and must be warmed before lay-up. Remove pre-cut sections from freezer and allow warming to ambient temperature (about 30 minutes). The plastic bag and film MUST BE INSPECTED for condensation or any evidence of moisture inside the bag. Moisture presence on the inside of the storage bag after thawing is cause for rejection of the material.

3. Peel ONE SIDE ONLY of protective backing film. Do Not Touch Center of Film!

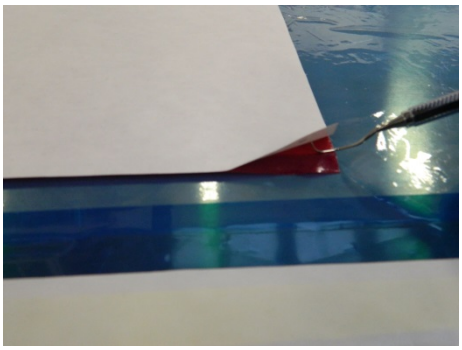

4. Lay film on lower wedge test plate, aligning it with the edge of the blue flash breaker tape. Do not overlap blue flash breaker tape. Smooth out any wrinkles or air pockets by pulling the film from the edges only.

5. Remove top layer of protective backing from the adhesive film and lay the positioning cloth material on the adhesive. Ensure the cloth extends a minimum of 1/2″ beyond each side of the plate to assist gas diffusion out of the adhesive film during cure.

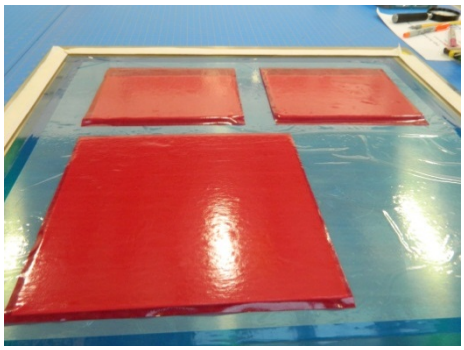
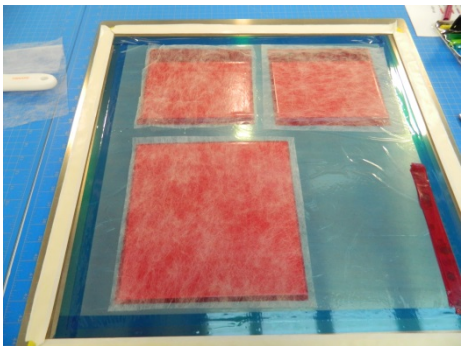

6. Lay the top plate (PAA) on the adhesive film. Visually check that upper and lower plates are aligned. Secure with additional blue flash breaker tape, as needed, to avoid shifting during the vacuum process.


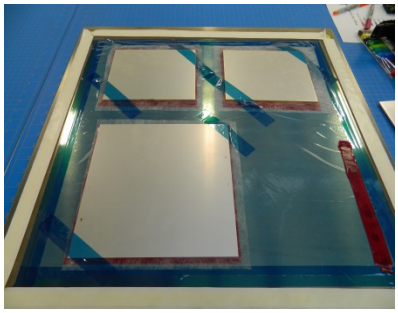
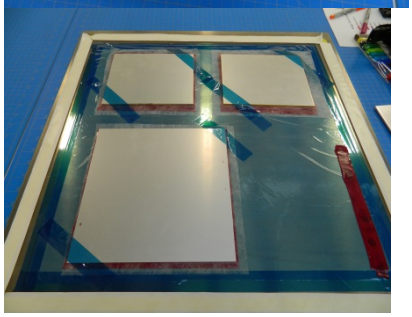

7. Proceed with the steps for layup of the lap shear test specimens.

A-6.3 LAP SHEAR TEST SPECIMEN LAYUP

1. Offset a single 9″ x 9″ panel to one side of the caul plate as shown in the above pictures, with the primer side facing up.

2. Thaw one 9″ x 9″ pre-cut adhesive film (3M AF-163-2 -Red) prior to use. Remove pre-cut sections from freezer and allow warming to ambient temperature. The plastic bag and film MUST BE INSPECTED for condensation or any evidence of moisture. Moisture inside the bag after thawing is cause for rejection of the material.

3. Peel the protective backing layer from ONE SIDE ONLY of the adhesive film and apply it to the metal plate as shown. Do not touch center of the film. Smooth out any wrinkles or air pockets by pulling on corners of the film.

4. After removing the top layer of the protective backing from the adhesive film, lay down the positioning cloth material on the adhesive. Ensure that the cloth extends a minimum of 1/2″ beyond each side of the plate to assist gas diffusion out of the adhesive film during cure.

5. Lay the top plate on the adhesive film. Visually check that the upper and lower plates are aligned. Secure with additional blue flash breaker tape to prevent shifting during the vacuum process.

A-6.4 FINALIZE LAYUP OF WEDGE AND SHEAR TEST SPECIMENS

1. Peel back a small section of paper backing from the yellow barrier sealing tape and install four thermocouples to the designated locations shown in the diagram below. Add one additional layer of barrier tape to seal around the thermocouple wires.

2. Apply flash breaker tape to the tip of the thermocouple wire to ensure the additional layers will not affect their placement.

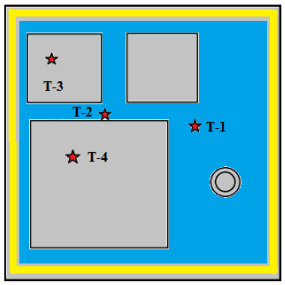

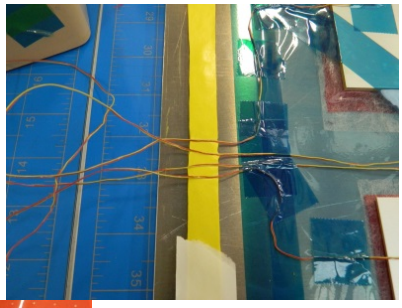

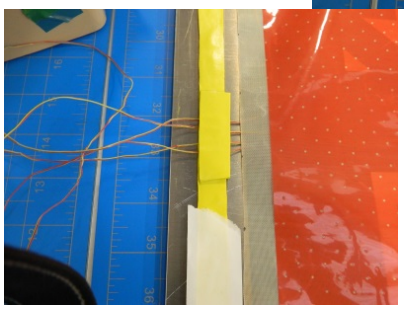

3. Cut and apply a layer of fiberglass peel ply to fit tightly inside of the tacky tape barrier. The peel ply should cover all three of the plates (two wedge specimens and one lap shear specimen).

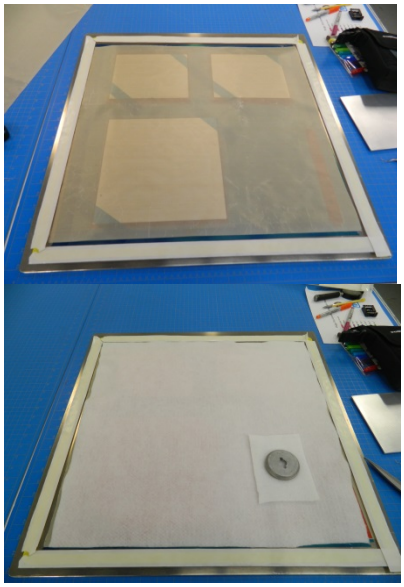

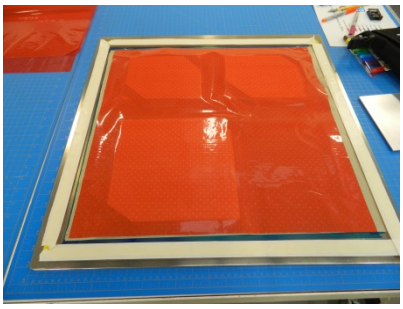

4. Cut and apply a layer of perforated red release film to the same dimensions as above peel ply and lay directly on top of the peel ply layer.

5. Cut and apply a layer of breather cloth of the same approximate dimensions as the perforated release film and peel ply. Lay the breather cloth directly on top of the other layers.

6. Cut an extra piece of breather cloth approximately 4″x 4″ for the vacuum port fitting. Place it in the area of the caul plate without a test specimen and center the vacuum port fitting on top of it.

7. Cut vacuum bag material to overlap the entire caul plate a minimum of 2″ on each side. The approximate dimensions of this bag are 26″ x 26″.

8. Peel off the white paper backing on the tacky tape around the perimeter of the plate. Apply one side of the bag to the tacky tape and firmly press down on the tape to attach the bag to the tape. Carefully pull the bag tight and lay the remainder of the bag down against the yellow tacky tape, smoothing the bag to avoid creating air gaps, folds, or wrinkles.

9. Smooth out all four sides of the vacuum bag and use a roller to ensure that the tacky tape is firmly attached to the bag. Look closely for trapped air bubbles and work them out with the roller or by hand.

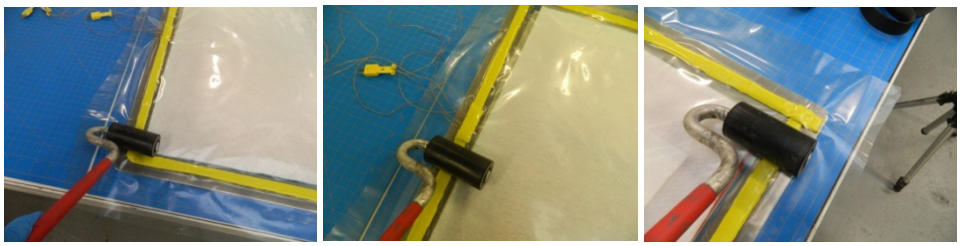

10. Once the bag is completely attached and secure, locate the vacuum port fitting and cut a small slit through the vacuum bag into the port opening. Hold the fitting in place and insert the male vacuum fitting into the port and gently tighten in place, being careful to not wrinkle the bag.

A-6.5 APPLY VACUUM AND PERFORM LEAK CHECK

1. Connect the vacuum source via the hose assembly to the port. The Venturi-type vacuum device is preferred because it has a much greater adjustment range than the vacuum pump.

2. Apply vacuum to achieve 10–11 inches mercury of vacuum per the gauges.

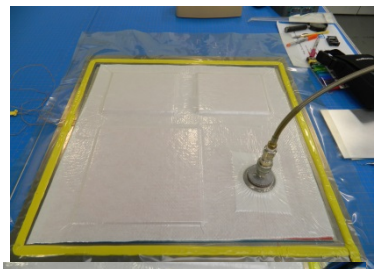

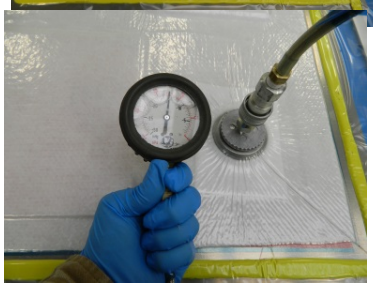

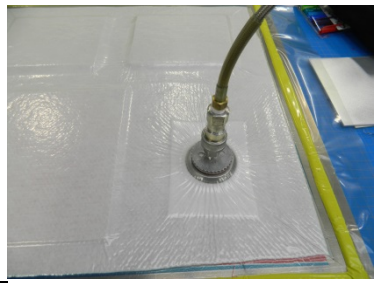

3. Tighten the vacuum port to ensure a good seal and no loss of vacuum.

4. Remove vacuum source and ensure leakage rate of less than 1 inch mercury per minute is maintained.

5. If vacuum cannot be maintained, find the source of the leak and seal it.

6. Once vacuum is ensured, caul plates are ready for oven cure.

A-7. OVEN-CURING PROCESS UNDER VACUUM, AF 163-2 FILM ASSEMBLIES

Treated test plates assembled with AF 163-2 adhesive film require a heat/vacuum cure process as noted:

1. Cure for 90 minutes after ramp-up is complete at 250°F +/- 10°F (121°C +/- 5.6°C). CAUL PLATE TEMPERATURE shall be used for parameter, not test specimen temperature.

2. Ramp-up rate of 3°F per minute and ramp-down rate of up to 10°F per minute is allowed.

3. Maintain 10–11 inches mercury vacuum during cure AND after heat cycle until plate temperature is less than 100°F.

4. Note the current temperature of the caul plate with the IR thermometer and confirm that the data logger is within +/-5°F.

5. Record cure profile data with the Omega data logger for the entire cure process, from initial ramp-up until plate temperature is less than 100°F after cool down.
   Best practice dictates periodic monitoring of the cure cycle to ensure all temperature and vacuum readings are maintained per specifications throughout the cure cycle.

A-8. CURING-OVEN OPERATION

1. Initiate switches for power, lights, fan, and heat during a warm-up sequence. On the oven controller digital display, scroll to “Adhesive Cure” profile and press “Enter.”

2. Heat the oven to a minimum of 75°F and no more than 100°F prior to loading the caul plate(s).

3. Connect the four thermocouples from the caul plates to the data logger through the access port on the oven side. Within the data logger setup, identify the batch lot number and use “Adhesive Cure” for retrieval of data on download. This will monitor and record ramp-up, cure, and ramp-down temperatures and time.

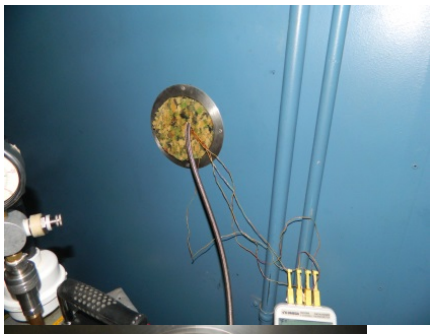

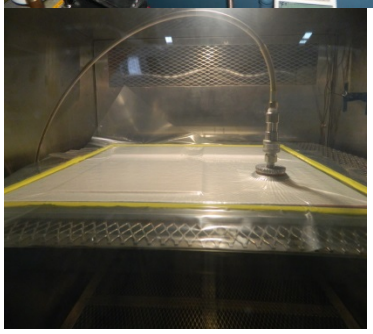

4. Connect the vacuum line and a vacuum monitor gage, one per caul plate, through the oven side ports.

5. Continue vacuum at 10–11 inches mercury and allow system to stabilize.

6. Securely latch door and verify that data logger is operational and has maintained temperature synchronization.

7. Initiate the adhesive cure profile heating run on the oven controller.

8. On completion of the heat cure cycle, continue vacuum operation until caul plates are less than 100°F. Open the oven door to help the cool-down of plates, approximately 45

minutes. Using the IR thermometer, verify that the plate temperature is <100°F prior to removal.

9. Remove the caul plates from the oven, disconnect the vacuum lines, and unbag the samples. Be careful not to damage the thermocouple wires when removing the sealing tape. Completely remove the plates from all remaining films, flash tape, and the caul plate.

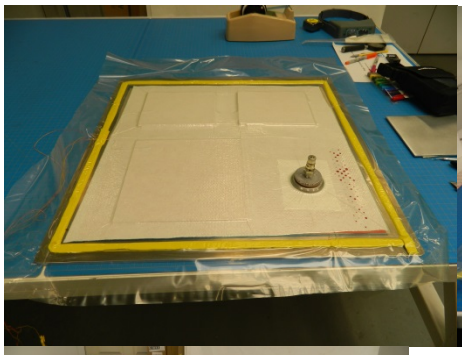


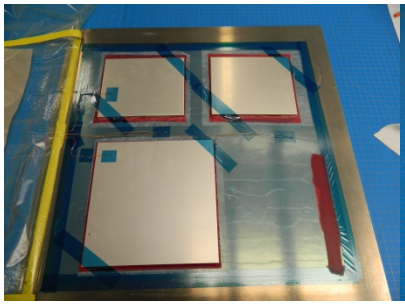
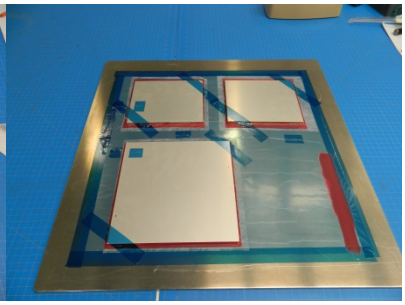

A-9. CUTTING PLATES

1. Cut the three plates to meet the criteria for testing listed in procedures ASTM D3762-98 and ATSM D3165-07.

2. One-inch and 1/2-inch cutting guides should be used during the cutting process. When installing them, confirm the distances from the blade to the guide with a tape measure.

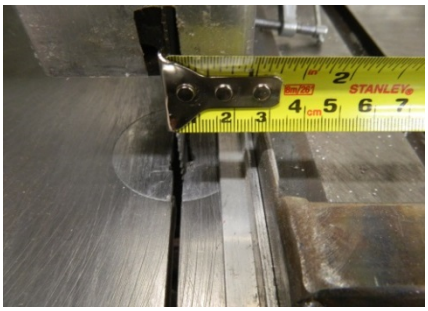

3. Prior to cutting edge drops, the bleed-out must be removed using a belt sander to ensure that a clean edge is present to allow straight cuts.

4. The wedge test samples should be cut in accordance with the following figures. A 1/2″ drop should be cut from each side of the 6″ edges to ensure nonuniform edge thickness is removed.

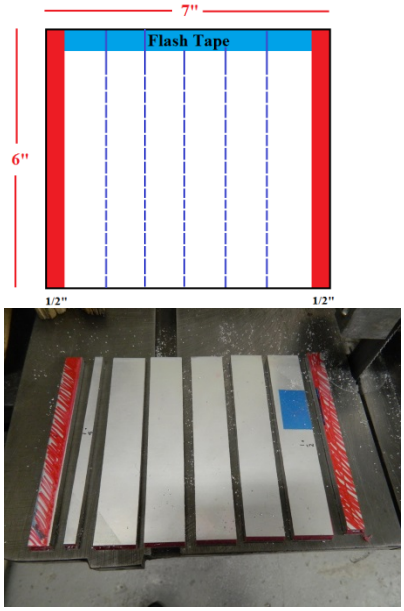

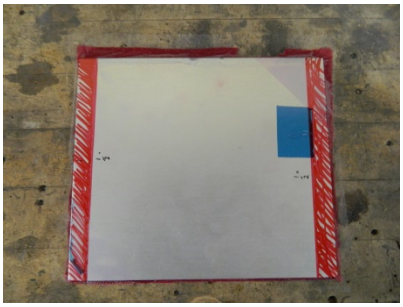

5. The lap shear plate should be cut in accordance with the following figures. A 1/2″ drop should be cut from the left and right sides to remove nonuniform thickness at the edges. A 1″ drop should be cut from the top and bottom side, creating an 8″ x 7″ plate.

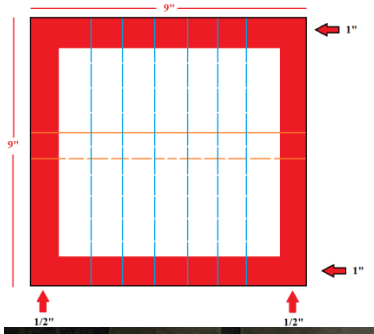

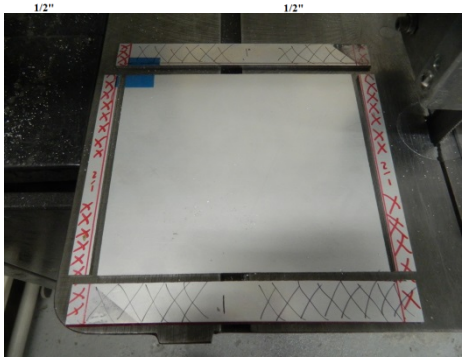

6. Kerfs should be cut into the lap shear plate to facilitate tensile strength testing on the load frame. One kerf is required on each side of the plate, with offsets that provide approximately 1″ space from kerf to kerf. NOTE: A 1/8″ drop on the 7″ may be required to fit in the table saw kerf fixture. This drop is performed on the sheet metal shear.

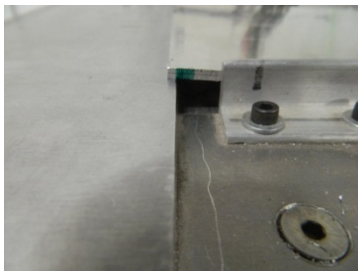

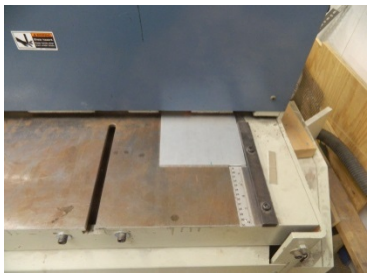

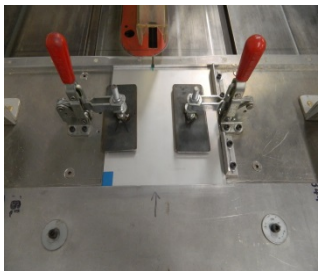

7. After all kerf lines and drop cuts have been made, the remaining plate should be cut into 1″ test specimens. Cut perpendicular to the flash tape on the wedge samples and perpendicular to the kerf lines on the lap shear samples.

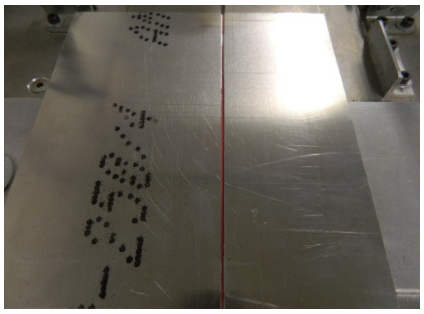
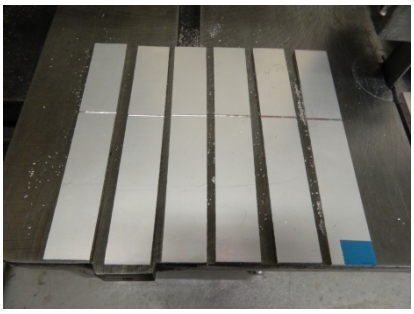

8. Using the belt sander, smooth out each side of the samples to aid in bond line thickness measurement.

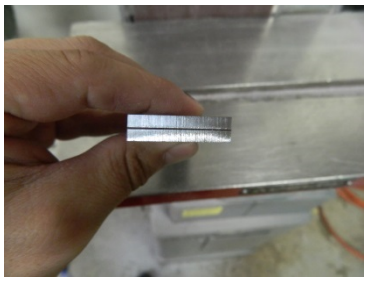

A-10. BOND LINE THICKNESS MEASUREMENTS

Bond line thickness measurements are made prior to initiating the ASTM strength testing procedures utilizing the Dino-lite LED microscope. The instrument shall be calibrated in accordance with the owner's manual. Measurements of the bond line thickness shall be recorded on each of the specimens.

1. For the lap shear specimens, take five bond line measurements between the two kerf cuts and average them for the final bond line thickness measurement.

2. For the wedge test specimens, take five bond line measurements approximately 1″ below the flash tape area (the region of interest). Once the measurements have been taken, the average will be used for the final bond line thickness measurement.

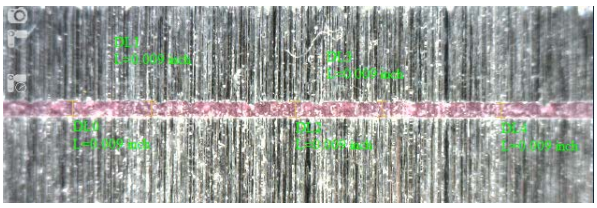

A-11. MARKING CRACK GROWTH ON WEDGE SPECIMENS

The wedge-driven crack will be monitored for growth. The following color chart is used to mark the crack growth from day to day. The color chart will be used as part of this process to maintain continuity for an individual set of specimens when multiple sets of bond runs are being tested at one time.

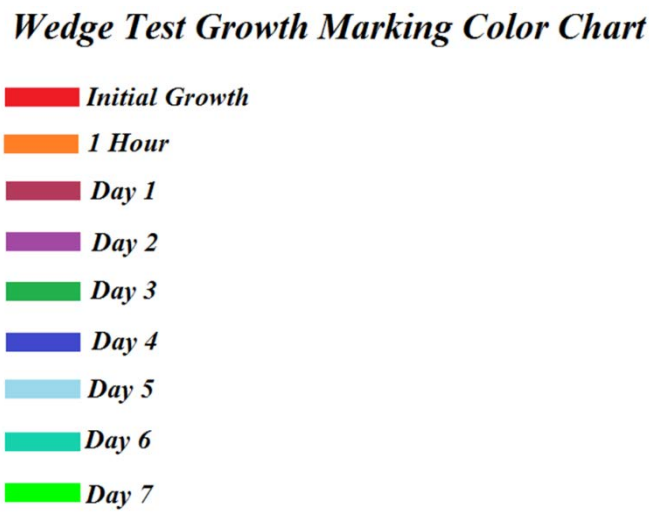

A-12. DATA COLLECTION OF STRENGTH TESTS

The data will be collected using Microsoft Excel running on a laptop computer. To minimize transcription errors, all data capturing is done on pre-loaded spreadsheets listed in the Bonding folder of the AANC laptop and can be found under MY COMPUTER, MY DOCS, BONDING. Screenshots of the data capturing forms are shown below.

Fabrication Date 17-18 Oct 2013	**Wedge Test Results**										
Date/Time of Measure											
Run/Sample Number	IG	1 HR	Day 1	Day 2	Day 3	Day 4	Day 5	Day 6	Day 7	Total	Failure Mode
BR-19-1	1.13"	.089"	.197"	.086"	0	0	0	0	0	1.539"	
BR-19-2	1.06"	.161"	.164"	.073"	.038"	0	0	.073"	0	1.636"	
BR-19-3	1.08"	.083"	.167"	.085"	.194"	0	0	0	0	1.65"	
BR-19-4	1.14"	.129"	.100"	0	0	0	0	0	0	1.381"	
BR-19-5	1.14"	.049"	0	0	.036"	0	0	0	0	1.262"	

Date: 15 November 2013	Lap Joint Pull Test				
Sample Number	Max Load (lbs)	Area (in^2)	PSI Load	Failure Mode	Bond Line Thickness (in)
BR-20-1	3940	1.22	3229.5	*Mixed	0.01
BR-20-2	3926	1.22	3218	*Mixed	0.009
BR-20-3	3937	1.21	3253.7	*Mixed	0.01
BR-20-4	3922	1.23	3188.6	*Mixed	0.011
BR-20-5	3977	1.22	3259.8	*Mixed	0.01
BR-20-6	4019	1.23	3267.4	*Mixed	0.01
BR-20-7	3944	1.23	3206.5	*Mixed	0.009
NOTE: * Primarily Cohesive Failure with some adhesive failure near kerf line.					

APPENDIX A

AUTHORIZED OPERATOR LIST

Name of Operator	**Signature of Operator**	**Date**	**Signature of Process Owner**
Name of Operator	**Signature of Operator**	**Date**	**Signature of Process Owner**
Name of Operator	**Signature of Operator**	**Date**	**Signature of Process Owner**
Name of Operator	**Signature of Operator**	**Date**	**Signature of Process Owner**
Name of Operator	**Signature of Operator**	**Date**	**Signature of Process Owner**
Name of Operator	**Signature of Operator**	**Date**	**Signature of Process Owner**
Name of Operator	**Signature of Operator**	**Date**	**Signature of Process Owner**
Name of Operator	**Signature of Operator**	**Date**	**Signature of Process Owner**
Name of Operator	**Signature of Operator**	**Date**	**Signature of Process Owner**
Name of Operator	**Signature of Operator**	**Date**	**Signature of Process Owner**
Name of Operator	**Signature of Operator**	**Date**	**Signature of Process Owner**
Name of Operator	**Signature of Operator**	**Date**	**Signature of Process Owner**

APPENDIX B—REFERENCES REVIEWED BUT NOT CITED IN PAPER

The listed citations were obtained from the Sandia National Laboratories Technical Library, the Federal Aviation Administration William J. Hughes Technical Center library, and other online sources as part of a comprehensive search for relevant papers. Abstracts from all citations in this report (i.e., those used and those ultimately excluded) were reviewed, a short synopsis was created, and a determination of the need for further review of the full paper was made. After reading in full the papers determined to warrant further review, they may or may not have been cited and included in the references section of this paper. The decision was based on an individual paper's relevance to the two topics of interest, specifically weak bond fabrication and nondestructive inspection for bond-strength measurement. This list of references was included because they are, although not cited, still relevant to this work.

B-1. Phillips, D.H., "Computational Chemistry of Adhesive Bonds," Langley Research Center, NASA Technical Reports Server, Document ID: 19990068472, 1999.

B-2. Nettles, A.T., "Permeability Testing of Composite Material and Adhesive Bonds for the DC-XA Composite Feedline Program," Marshall Space Flight Center, NASA Technical Reports Server, Document ID: 19950017131, 1995.

B.3 Jagasivamani, V. and Smith, A.C., "Assessing the Integrity of Structural Adhesive Bonds by the Measurement of Acoustic Properties," Langley Research Center, NASA Technical Reports Server, Document ID: 19930035591, 1992.

B-4. American Society for Nondestructive Testing, Inc. & NASA, "NDE of Adhesive Bonds and Bondlines; Proceedings of the 1989 ASNT Fall Conference," Valley Forge, PA, Oct. 9-13, Document ID: 19910032203, 1989, p. 160.

B-5. Thomann, D.G., "Testing Adhesive Bonds to Cloths," Johnson Space Center, NASA Technical Reports Server, Document ID: 19870000414, 1987.

B-6. Mall, S. and Johnson, W.S., "Characterization of Mode I and Mixed-Mode Failure of Adhesive Bonds Between Composite Adherends," Langley Research Center, NASA Technical Reports Server, Document ID: 19860056330, 1986.

B-7. Guertin, L.J., Billington, K.L., and Ward, V.R., "Reducing the Resistance of Conductive-Adhesive Bonds," Johnson Space Center, NASA Technical Reports Server, Document ID: 19830000219, 1983.

B-8. Keir, A.R. and Dominguez, X.A., "Tool Severs Hidden Adhesive Bonds," Johnson Space Center, NASA Technical Reports Server, Document ID: 19820000322, 1983.

B-9. Johns, J.M. and Reed, M.W., "Heat-Shrinkable Film Improves Adhesive Bonds," Johnson Space Center, NASA Technical Reports Server, Document ID: 19790000429, 1980.

B-10. Hahn, C., “Strength Behavior of Adhesive Bonds Under Impact Loads,” NASA Technical Reports Server, Document ID: 19740024876, 1974.

B-11. Frank, L. and Schmitz, G., “Dot Patterns Provide Reproducible Flaw Areas for Study of Adhesive Bonds,” NASA Technical Reports Server, Document ID: 19660000366, 1966.

B-12. NASA Tech Brief 65-10173, “Peel Resistance of Adhesive Bonds Accurately Measured,” Goddard Space Flight Center, NASA Technical Reports Server, Document ID: 19650000171, 1965.

B-13. Black, J.M. and Blomquist, R.F., “Relationship of Polymer Structure to Thermal Deterioration of Adhesive Bonds in Metal Joints,” NASA Technical Reports Server, Document ID: 19890068240, 1959.

B-14. Black, J.M. and Blomquist, R.F., “Relationship of Metal Surfaces to Heat-Aging Properties of Adhesive Bonds,” NASA Technical Reports Server, Document ID: 19930085114, 1958.

B-15. Hou, T.H., Miner, G.A., Lowther, S.E., Connell, J.W., and Baughman, J.M., “Environmental Aging of Scotch-Weld (TradeMark) AF-555M Structural Adhesive in Composite to Composite Bonds,” Langley Research Center, NASA Technical Reports Server, Document ID: 20100021071, 2010.

B-16. Ojeda, C.E., Oakes, E.J., Hill, J.R., Aldi, D., and Forsberg, G.A., “Temperature Effects on Adhesive Bond Strengths and Modulus for Commonly Used Spacecraft Structural Adhesives,” Jet Propulsion Laboratory, NASA Technical Reports Server, Document ID: 20120007450, 2011.

B-17. Lynch III, D.A. and Ludwiczak, D.R., “Shear Strength Analysis of the Aluminum/Ice Adhesive Bond,” Glenn Research Center, NASA Technical Reports Server, Document ID: 19960029316, 1996.

B-18. Davis, G.D., Ahearn, J.S., Matienzo, L.J., and Venables, J.D., “Use of Hydration Inhibitors to Improve Bond Durability of Aluminum Adhesive Joints,” NASA Technical Reports Server, Document ID: 19860001784, 1985.

B-19. Koch, R.O., “Effects of Processing Variables on Bond Strength of Polyurethane Adhesive,” NASA-CR-61808, NASA Technical Reports Server, Document ID: 19680016819, 1967.

B-20. Lee, S.Y., “Fluoroepoxy Adhesives Bond Fluoroplastics,” Goddard Space Flight Center, NASA Technical Reports Server, Document ID: 19890000065, 1989.

B-21. Lee, S.Y., “The use of Fluoroepoxy Compounds as Adhesives to Bond Fluoroplastics Without any Surface Treatment,” Goddard Space Flight Center, NASA Technical Reports Server, Document ID: 19880054323, 1989.

B-22. Davidson, J.R., “Shear Strength at 75 F to 500 F of Fourteen Adhesives Used to Bond a Glass-Fabric-Reinforced Phenolic Resin Laminate to Steel,” NACA-TN-3901, NASA Technical Reports Server, Document ID: 19930084782, 1956.

B-23. Bartosz, K., “Hemivariational Inequalities Modeling Dynamic Contact Problems With Adhesion,” *Nonlinear Analysis, Theory, Methods & Applications*, Vol. 71, No. 5–6, 2009, pp. 1747–1762.

B-24. Nassar, S.A., Andrews, K.T., Kruk, S., and Shillor, M., “Modelling and Simulations of a Bonded Rod,” *Mathematical and Computer Modelling*, Vol. 42, Issue 5–6, 2005, pp. 553-572.

B-25. Xu, L.R., Sengupta, S., and Kuai, H., “An Experimental and Numerical Investigation of Adhesive Bonding Strengths of Polymer Materials,” *International Journal of Adhesion and Adhesives*, Vol. 24, No. 6, 2004, pp. 455–460.

B-26. Li, J., Guymon, S.L., “Robust Metal to Composite Hybrid Bonded Joint,” *AHS International 60th Annual Forum Proceedings*, Vol. 42, No. 5–6, 2004, pp 553–572.

B-27. Uddin, M.A., Chan, Y., Chan, H.P., and Alam, M.O., “A Continuous Contact Resistance Monitoring during the Temperature Ramp of Anisotropic Conductive Adhesive Film Joint,” *Journal of Electronic Materials*, Vol. 33, No. 1, 2004, pp. 14–21.

B-28. Chau, O., Shillor, M., and Sofonea, M., “Dynamic Frictionless Contact With Adhesion,” *Zeitschrift fur Angewandte Mathematik und Physik*, Vol. 55, No. 1, 2004, pp. 32–47.

B-27. Wienhold, P.D., “The Effect of Shelf Life on the Bond Strength of Etched Filled PTFE PC Board Materials,” *Proceedings of the 46th International SAMPE Symposium and Exhibition*, Long Beach, CA, 2001.

B-28. Xu, L.R. and Rosakis, A.J., “Real Time Experimental Investigation of Dynamic Failure Mode Selection in Sandwich Structures,” *Mechanics of Sandwich Structures; Proceedings of the Symposium, 2000 ASME International Mechanical Engineering Congress and Exposition*, Orlando, FL, 2000.

B-29. Duthinh, D., “Tensile Strength of an Interlocking Composite Connection,” Monograph PB2001-100494, National Institute of Standards and Technology, Building and Fire Research Lab, Gaithersburg, MD, 2000.

B-30. Geymonat, G., Krasucki, F., and Lenci, S., “Mathematical Analysis of a Bonded Joint With a Soft Thin Adhesive,” *Mathematics and Mechanics of Solids*, Vol. 4, No. 2, 1999, pp. 201–225.

B-31. Arnott, D.R., Rider, A.N., Olsson-Jacques, C.L., Lambrianidis, et al., "Bond Durability Performance—The Australian Silane Surface Treatment," *21st ICAS Congress*, Melbourne, Australia, 1998.

B-32. Arnold, J.R., Sanders, C.D., Sanders, D., et al., "A Study of Titanium Surface Pretreatments for Bonding with Polyimide and Epoxy Adhesives," *Proceedings of the 29th International SAMPE Technical Conference*, Orlando, FL, 1997.

B-32. Shetty, S.P. and Spearing, S.M., "Fracture Resistance of a Fiber-Reinforced Film Adhesive," *Scripta Materialia*, Vol. 37, No. 6, 1997, pp. 787–792.

B-33. Heslehurst, R.B. and Baird, J.P., "Further Understanding of Aged Composite and Adhesively Bonded Structures," Nondestructive Evaluation of Aging Aircraft, Airports, and Aerospace Hardware; Proceedings of the Meeting, Scottsdale, AZ, 1996.

B-34. Hart-Smith, L.J., Redmond, G., Davis, M.J., "The Curse of the Nylon Peel Ply," *Materials and Process Challenges: Aging Systems, Affordability, Alternative Applications*. Vol. 41–I; Anaheim, CA, 1996.

B-35. Myers, R.S., "Verification of Surface Preparation for Adhesive Bonding," NASA Marshall Space Flight Center, *Aerospace Environmental Technology Conference*, Huntsville, AL, 1994.

B-36. Lai, S. and Zou, X., "Study on Simulative Flying Effects Testing for High Performance Adhesive Bonding Honeycomb Structure," *Materials Challenge Diversification and the Future, Proceedings of the 40th International SAMPE Symposium and Exhibition*, Anaheim, CA, 1995.

B-37. Zanni-Deffarges, M.P., Shanahan, M.E.R., "Evaluation of Adhesive Shear Modulus in a Torsional Joint: Influence of Ageing," International Journal of Adhesion and Adhesives Vol. 13, No. 1, 1993, pp. 41-45.

B-38. Saatchi, H., Durako, B., Reynolds, D., Dost, E., Willden, K., et al., "In Situ Processing Methods for Composite Fuselage Sandwich Structures," NASA. Langley Research Center, Third NASA Advanced Composites Technology Conference, Vol. 1, Part 2, 1993, pp. 537–546 (See N95-28823 10-24).

B-39. Sugama, T., Carciello, N.R., Miura, M., "Adhesion of Crystalline Polyphenylethereth erketone (PEEK) in Metal-to-Metal Joints," International Journal of Adhesion and Adhesives, Vol. 12, 1992, pp. 27–37.

B-40. Chin, J.W., Wightman, J.P., "Surface Characterization and Adhesion of Oxygen Plasma-Modified LARC-TPI," SAMPE Quarterly, Vol. 23, 1992, pp. 2–10.

B-41. Alves, M., “Analysis of Composite Materials Subjected to a Unilateral Contact Condition With Adhesion on the Interface of its Constituents,” Ph.D. Thesis, University of Michigan, Ann Arbor, MI, 1991.

B-42. De Gennes, P.G., “Simple Views on Adhesion and Fracture,” Canadian Journal of Physics, Vol. 68, 1990, pp. 1049–1053.

B-43. Jiao, D., “Ultrasonic Oblique Incidence Interface Characterization,” Ph.D. Thesis, Drexel University, Philadelphia, PA, 1990.

B-44. Maguire, D.M., “Joining Thermoplastic Composites,” SAMPE Journal, Vol. 25, 1989, pp. 11–14.

B-45. Pavlov, V.I., Galich, V.D., “Fracture Parameters of Adhesive Joints Under Symmetric Debonding,” Mekhanika Kompozitnykh Materialov, 1988, pp 996–1000.

B-46. Jortner, J., Pfeifer, W.H., “Experimental Study of Fracture, Deformation and Failure Modes of Threaded Joints Between 2D and 3D Carbon—Carbon Composites,” Thermostructural Behavior of Carbon-Carbon Composites, Anaheim, CA, 1986.

B-47. Stoller, H.M., Allred, R.E., “Effect of Argon Plasma Pretreatment on Amination of Polyaramid Filaments,” Materials for Space—the Gathering Momentum, Seattle, WA, 1986.

B-48. Lagace, P.A, Allen, M.W., “Evaluation of the Alternative Manufacturing Methods for Bonding Graphite/Epoxy Composites,” Advancing Technology in Materials and Processes, Anaheim, CA, 1985.

B-49. Hart-Smith, L.J., Thrall, E.W., “Structural Analysis of Adhesive-Bonded Joints,” Structural Analysis of Adhesive-Bonded Joints, 1985, pp. 241–321.

B-50. Hart-Smith, L.J., “Effects of Flaws and Porosity on Strength of Adhesive-Bonded Joints,” Technology Vectors, Reno, NV, 1984.

B-51. Brockmann, W., Hennemann, O.D., Kollek, H., “Failure Mechanisms in the Boundary Layer Zone of Metal/Polymer Systems,” Adhesive Joints, K.L. Mittal, ed., Springer, 1984, pp. 469–484.

B-52. Buckley, D.H., Surfaces (Characterization of Surface Properties for Predicting Bond Quality),” National Aeronautics and Space Administration. Lewis Research Center, Cleveland, OH, 1983.

B-53. Hennemann, O.D. and Brockmann, W., “Weak Boundary Zones in Metal Bonds,” Material and Process Advances `82, Atlanta, GA, 1982.

B-54. Stone, M.H., "The Effect of Adhesive Properties on the Low Temperature Strength of Joints Between Metals and Carbon Fibre-Reinforced Plastics," *International Journal of Adhesion and Adhesives*, Vol. 1., 1981.

B-55. Kinloch, A.J., "The Science of Adhesion I - Surface and Interfacial Aspects," *Journal of Materials Science*, Vol. 15, 1980, pp. 2141–2166.

B-56. Rose, J.L., Thomas, G.H., "An Adhesive Bond Strength Prediction Algorithm Based on Ultrasonic Signal Analysis," *International Journal of Adhesion and Adhesives*, Vol. 1, 1980, pp. 29–33.

B-57. Baun, W.L., "Failure Mechanisms and Interphase Chemistry of Gold Films on TI6AL4V. Part 1: Surface Chemistry of Failure Surfaces," Final Report, 1980.

B-58. Rose, J.L. and Thomas, G.H., "Ultrasonic Procedures for the Determination of Bond Strength," Document No.: AFOSR-TR-78-0843, Drexel University, Mechanical Engineering & Mechanics Department, Philadelphia, PA, 1978.

B-59. Levine, S.R., "Adhesive/Cohesive Strength of a ZrO2.12 w/o Y2O3NiCrAlY Thermal Barrier Coating," *American Ceramic Society, Annual Meeting, 80th*, Detroit, MI, 1978.

B-60. Dreyfuss, P., Gent, A.N., and Runge, M.L., "Effect of Interfacial Chemical Bonding on the Strength of Adhesion of Glass-Polybutadiene Joints," Akron University, Ohio Institute of Polymer Science, Publication No. AD-A044505, 1977.

B-61. Robertson, R.E., "The Strength of an Adhesive Weak Boundary Layer (Polystyrene Sandwiched Between Polymethyl Methacrylate)," *Journal of Adhesion*, Vol. 7, 1975, pp. 121–136.

B-62. Nakao, K. and Sawada, S., "Research on Adhesion of Polyolefines (Adhesion Strength of Polyethylene Layer on Aluminum Foil)," Translated Into English from *Journal of the Adhesives Society of Japan*, Vol. 6, No. 4, 1970, pp 41–47.

B-67. Hart-Smith, L.J., "Adhesive-Bonded Scarf and Stepped-Lap Joints," NASA-CR-112237, 1973, 123 p.

B-68. Lohr, J.E., "Factors Affecting the Survivability of Stressed Bonds in Adverse Environments," *New Horizons in Materials and Processing; Proceedings of the Eighteenth National Symposium and Exhibition*, Los Angeles, CA, 1973.

B-69. Richmond, M.A., Aghajanian, M.K., McCormick, A.L., Waggoner, W.M., and Schultz, B.E., "Methods for Making Composite Bonded Structures," U.S. Patent Publication No.: US6863759, 2002.

B-70. Mehrabadi, F.A., "Experimental and Numerical Failure Analysis of Adhesive Composite Joints," *International Journal of Aerospace Engineering*, Vol. 2012, Article ID 925340, 2012, 10 p.

B-71. Baker, A.A., "A Proposed Approach for Certification of Bonded Composite Repairs to Flight-Critical Airframe Structure," *Applied Composite Materials (Netherlands)*, Vol. 18, No. 4, 2011, pp. 337–369.

B-72. Tserpes, K.I., Ruzek, R., Mezihorak, R., Labeas, G.N., and Pantelakis, S.G., "The Structural Integrity of a Novel Composite Adhesively Bonded Flap-Track Beam," Composite Structures (UK), Vol. 93, No. 8, 2011, pp. 2049–2059.

B-73. Bala Krishna Murthy, V., Venkata Kiran Kumar, R., Suresh Kumar, J., and Vijaykumar Reddy, K., "Fracture Analysis of Adhesively Bonded Single Lap Joint With Four Layered +thetas/-thetas] S Adherents," *International Journal of Applied Engineering Research* (India), Vol. 1, No. 4, 2011, pp. 951–960.

B-74. Katnam, K.B., Crocombe, A.D., Khoramishad, H., and Ashcroft, I.A., "The Static Failure of Adhesively Bonded Metal Laminate Structures: A Cohesive Zone Approach," *Journal of Adhesion Science and Technology (Netherlands)*, Vol. 25, No. 10, 2011, pp. 1131–1157.

B-75. Sim, N.W., Mustapha, F., Varatharajoo, R., Zahari, R., and Majid, D.L., "Parametric Study on Cohesive Element for Composite Fuselage Model," Vol. 471–472, 2011, pp. 1085–1090.

B-76. Wang, J., Stankiewicz, M., Zhou, Z., Baker, A., and Chiu, W.K., "Battle Damage Repair of a Helicopter Composite Frame-to-Skin Junction—A Sole External Repair Approach," *Composite Structures (UK)*, Vol. 92, No. 4, 2010, pp. 936–949.

B-77. Fundeanu, I., Klee, D., Kwakernaak, A., and Poulis, J.A., "The Effect of Substituted Poly (p-xylene) on the Quality of Bonded Joints When Used as a Primer Replacement," *International Journal of Adhesion and Adhesives (UK)*, Vol. 30, No. 2, 2010, pp. 111–116.

B-78. Banea, M.D. and da Silva, L.F.M., "The Effect of Temperature on the Mechanical Properties of Adhesives for the Automotive Industry," *Proceedings of the Institution of Mechanical Engineers, Part L (Journal of Materials: Design and Applications)*, Vol. 224, No. L2, 2010, pp. 51–62.

B-79. Yan L., Yong, M.H., Ying, C.L., You, S.Q., and Jiao, T.D., "Analysis of Bonding Stress With High Strength Adhesive Between the Reflector and the Mounts in Space Camera," *Proceedings of The International Society for Optical Engineering*, Vol. 7654, 2010, 6 p.

B-80. Masserey, B., Kostson, E., and Fromme, P., "Monitoring of Fatigue Crack Growth Using Guided Ultrasonic Waves," *Proceedings of The International Society for Optical Engineering*, Vol. 7647, 2010, 9 p.

B-81. Flinn, E.D., "NASA Coating Helps Keep Hearts Beating," Aerospace America, Vol. 47, No. 9, 2009, pp. 22–23.

B-82. Zadpoor, A.A., Sinke, J., and Benedictus, R., "The Mechanical Behavior of Adhesively Bonded Tailor-Made Blanks," *International Journal of Adhesion and Adhesives (UK)*, Vol. 29, No. 5, 2009, pp. 558–571.

B-83. Soon H.Y., Kwan H.L., Dai G.L., and Byoung J.K., "Durability Improvement of Co-Cured Carbon/Epoxy Composite-Aluminum Laminate With Nano-Size Carbon Black at Cryogenic Temperature," *Journal of Adhesion Science and Technology (Netherlands)*, Vol. 23, No. 4, 2009, pp. 649–659.

B-84. Chadegani, A., Yang, C., and Dan-Jumbo, E., "Strain-Energy Release Rate Analysis of Adhesive-Bonded Composite Joints With Prescribed Interlaminar Crack," *Journal of Aircraft*, Vol. 46, No. 1, 2009, pp. 203–215.

B-85. Kostson, E. and Fromme, P., "Fatigue Crack Growth Monitoring in Multi-Layered Structures Using Guided Ultrasonic Waves," *Journal of Physics: Conference Series (UK)*, Vol. 195, No. 1, 2009, pp. 3–12.

B-86. Bellucci, S., Micciulla, F., Sacco, I., De Bellis, G., and Rinaldi, G., "Mechanical and Electrical Characterization of Epoxy Nanocomposites for Electromagnetic Shielding Devices in Aerospace Applications," *2009 IEEE International Symposium on Electromagnetic Compatibility*, 2009, pp. 89–96.

B-87. Bachir Bouiadjra, B., Fekirini, H., Belhouari, M., and Serier, B., "Numerical Analysis of the Behaviour of Repaired Inclined Cracks With Bonded Composite Patch Having Two Adhesive Bands in Aircraft Structures," Vol. 222, No. G7, 2008, pp. 963–968.

B-88. Stoyanov, P., Rodriguez, N., Dickinson, et al., "Evaluation of Advanced Adhesives for Aerospace Structures," *Journal of Materials Engineering and Performance*, Vol. 17, No. 4, 2008, pp 460–464.

B-89. Kilroy, J.P., Bradaigh, C.O., and Semprimoschnig, C.O.A., "Mechanical and Physical Evaluation of New Carbon Fibre/PEEK Composites for Space Applications," *SAMPE Journal*, Vol. 44, No. 3, 2008, pp. 22–34.

B-90. Shahin, K., Kember, G., and Taheri, F., "An Asymptotic Solution for Evaluation of Stresses in Balanced and Unbalanced Adhesively Bonded Joints," *Mechanics of Advanced Materials and Structures*, Vol. 15, No. 2, 2008, pp. 88–103.

B-91. Petrie, E.M., "Adhesives for the Assembly of Aircraft Structures and Components," *Metal Finishing*, Vol. 106, No. 2, 2008, pp. 26–31.

B-92. Prabhune, S.C. and Talreja, R., "Assessment of Adhesively Bonded Joints Subjected to Surface Damage by Paint Removal," *Aircraft Engineering and Aerospace Technology*, Vol. 79, No. 4, 2007, pp. 360–374.

B-93. Okafor, A.C. and Bhogapurapu, H., "Design and Analysis of Adhesively Bonded Thick Composite Patch Repair of Corrosion Grind-Out and Cracks on 2024 T3 Clad Aluminum Aging Aircraft Structures," *Composite Structures (UK)*, Vol. 76, No. 1–2, 2006, pp. 138–150.

B-94. Bhowmik, S., Bonin, H.W., Bui, V.T., and Weir, R.D., "Durability of Adhesive Bonding of Titanium in Radiation and Aerospace Environments," *International Journal of Adhesion and Adhesives*, Vol. 26, No. 6, 2006, pp. 400–405.

B-95. Taib, A.A., Boukhili, R., Achiou, S., Gordon, S., and Boukhili, H., "Bonded Joints With Composite Adherends. Part I. Effect of Specimen Configuration, Adhesive Thickness, Spew Fillet and Adherend Stiffness on Fracture," *International Journal of Adhesion and Adhesives*, Vol. 26, No. 4, 2006, pp. 226–236.

B-96. Anonymous, "Mechanical Properties and Performance of Engineering Ceramics and Composites II," *A Collection of Papers Presented at the 30th International Conference on Advanced Ceramics and Composites*, INSPEC:9397306, 2006, 784 p.

B-97. Latini, V., Striano, V., Venditti, F., Coppola, G., and Rendina, I., "Fiber Optic Health Monitoring System for Aerospace Hot Structures," *5th European Workshop on Thermal Protection Systems and Hot Structures*, 2006, 8 p.

B-98. dos Reis, H.L.M., and Kautz, H.E., "Nondestructive Evaluation of Adhesive Bond Strength Using the Stress Wave Factor Technique," *Journal of Acoustic Emission*, Vol. 5, No. 4, 1986, pp. 144–147.

B-99. Adams, D., DeVries, L., and Child, C., "Durability of Adhesively Bonded Joints for Aircraft Structures," *Technical Review Presented to Joint Advanced Materials and Structures Center of Excellence*, 2012, 25 p.

B-100. Zhu, Y. and Kedward, K., "Methods of Analysis and Failure Predictions for Adhesively Bonded Joints of Uniform and Variable Bondline Thickness," DOT/FAA/AR-05/12 Final Report, 2005, 61 p.

B-101. Tomblin, J., Strole, K., Dodosh, G., and Ilcewicz, L., "Assessment of Industry Practices for Aircraft Bonded Joints and Structures," DOT/FAA/AR-05/13 Final Report, 2005, 243 p.

B-102. Davis, M. and Tomblin, J., "Best Practice in Adhesive Bonded Structures and Repairs," DOT/FAA/AR-TN06/57, 2007, 58 p.

B-103. Reynolds, W.N. and Wilkinson, S.J., "The Analysis of Fibre-Reinforced Porous Composite Materials by the Measurement of Ultrasonic Wave Velocities," *Ultrasonics*, Vol. 41, 1978, pp. 159–163.

B-104. Powell, G.L., Smyrl, N.R., Janke, C.J., Wachter, et al., "Nondestructive Inspection of Graphite-Epoxy Laminates for Heat Damage Using Drift and LPF Spectroscopies," *In Proceedings, Conference on Characterization and NDE of Heat Damage in Graphite Epoxy Composites NTIAC*, Austin, TX, 1993, pp. 97–111.

B-105. Tracey, A.C., Morasch, J.T., Capps, A., and Flinn, B.D., "Potential Composite Bond Contamination by Contact Angle Fluids," SAMPE, 2013, 14 p.

B-106. Jeenjitkaew, C., Luklinska, Z., Guild, F., "Morphology and Surface Chemistry of Kissing Bonds in Adhesive Joints Produced by Surface Contamination," *International Journal of Adhesion and Adhesives*, Vol. 30, 2010, pp. 643–653.